Per. Mineral. (1999), *68*, 3, 231-260

PERIODICO di MINERALOGIA
established in 1930

An International Journal of
MINERALOGY, CRYSTALLOGRAPHY, GEOCHEMISTRY, ORE DEPOSITS, PETROLOGY, VOLCANOLOGY
and applied topics on *Environment, Archaeometry* and *Cultural Heritage*

Geochronology, Sr-Nd isotope geochemistry and petrology of Late-Hercynian dyke magmatism from Sarrabus (SE Sardinia)

SARA RONCA[1]*, ALDO DEL MORO[2] and GIANBOSCO TRAVERSA[1]

[1] Dipartimento di Scienze della Terra, Università di Roma "La Sapienza", P.le A. Moro 5, I-00185 Roma, Italy
[2] Istituto di Geocronologia e Geochimica Isotopica CNR, Pisa, Italy

Submitted, July 1999 - Accepted, November 1999

ABSTRACT. — Late-Hercynian dyke swarms of Sarrabus (southern Sardinia) consist of metaluminous up to peraluminous felsic products, prevalently rhyolitic in composition (granite porphyries, microgranites and aplites) and basic and intermediate dykes comprising few tholeiitic basalts and a calc-alkaline suite dominated by basaltic andesites and andesites. New geochronological data contribute to define the time-span of dyke magmatism. Rb-Sr mica ages for rhyolitic rocks cluster around 290 Ma and 270 Ma. Field data and one Rb-Sr biotite age (259 ± 3 Ma) obtained on a basaltic andesite sample indicate that mafic dykes prevalently intruded later than the felsic ones.

Mafic dyke rocks are mantle-derived, but, both among tholeiitic dykes and calc-alkaline ones, rocks representative of primary mantle melts are lacking. The least evolved calc-alkaline rocks are represented by rare basalts and by high-Mg basaltic andesites. Petrography, mineral and whole-rock chemistry, Sr and Nd isotopic features and mass balance calculations suggest that fractional crystallization associated with minor amount of crustal contamination controlled the evolution of the calc-alcaline suite. A model involving fractional crystallization and assimilation of metasedimentary materials (AFC) is proposed to account for the main geochemical and Sr and Nd isotopic variations from the high-Mg basaltic andesites to dacites. Tholeiitic basalts and the least evolved calc-alkaline rocks show an arc-type incompatible element signature (LILE and LREE enrichments and Ti, Nb, P depletions), positive $\varepsilon^{t}Sr$ and negative $\varepsilon^{t}Nd$ values suggesting derivation from a mantle source possibly enriched during a previous subduction event.

Differences in the Sr and Nd isotopic composition, in agreement with mineralogy and geochemistry, point to the occurrence of two different types of felsic dykes, i.e. the peraluminous (PR) and metaluminous to mildly peraluminous (MmPR) groups. It is proposed that PR dykes originated by partial melting from pelitic metasedimentary sources. The high $(^{87}Sr/^{86}Sr)_t$ ratios (0.7154 ÷ 0.7173) and the negative $\varepsilon^{t}Nd$ values (–7.4) shown by this group of rhyolites match those of the metasediments from the Hercynian basement of Sardinia. Mass balance calculations indicate that only the least silicic MmPR rhyolites could be genetically related to the basic-intermediate dykes by fractional crystallization relationships. On the contrary, for most MmPR rocks, an origin by partial melting of crustal souces seems more likely. Their relatively low $(^{87}Sr/^{86}Sr)_t$ and high $\varepsilon^{t}Nd$ values (0.7076 ÷ 0.7089 and –5.7 ÷ –6.3, respectively), partly overlapping those of the calc-alkaline basic-intermediate dykes, require source materials characterized by a less evolved Nd and Sr isotopic composition than those observed for the Sardinia

* Corresponding author, E-Mail: ronca@uniroma1.it

metamorphic basement and imply the involvement of both crustal and juvenile mantle components.

RIASSUNTO. — Il magmatismo filoniano tardo-ercinico del Sarrabus (Sardegna sudorientale) è rappresentato da prodotti felsici da metalluminosi a peralluminosi, a prevalente composizione riolitica (porfidi granitici, micrograniti e apliti) e da filoni basici e intermedi. Questi ultimi comprendono pochi basalti tholeiitici e una suite calcoalcalina in cui prevalgono termini andesitico-basaltici e andesitici. Nuovi dati geocronologici contribuiscono a definire l'intervallo di tempo in cui il magmatismo filoniano si è sviluppato. Per i filoni riolitici, le età Rb-Sr su muscovite e biotite si concentrano intorno a 290 Ma e a 270 Ma. I dati geologici e un'età su biotite (259± 3 Ma), ottenuta su un dicco di composizione andesitico-basaltica, suggeriscono che i filoni basici e intermedi si siano messi in posto successivamente a quelli felsici. Le rocce filoniane mafiche provengono da magmi basici di derivazione mantellica ma, né tra i filoni tholeiitici né in quelli calcoalcalini sono stati ritrovati termini rappresentativi di magmi primari. Le rocce calcoalcaline meno evolute sono rappresentate da rari basalti e da andesiti basaltiche ricche in Mg. I dati petrografici, i caratteri composizionali dei minerali e della rocce totali, le composizioni isotopiche di Sr e Nd e i bilanci di massa suggeriscono che l'evoluzione della suite calcoalcalina sia stata controllata da cristallizzazione frazionata associata a contaminazione crostale di modesta entità. Si propone un modello di cristallizzazione frazionata + assimilazione di materiale metasedimentario (AFC) per spiegare le principali variazioni geochimiche ed isotopiche osservate nell'ambito della suite calcoalcalina (da andesiti basaltiche ricche in Mg ad andesiti e daciti). I filoni basaltici tholeiitici e quelli meno evoluti della serie calcoalcalina mostrano andamenti degli elementi incompatibili che richiamano quelli dei magmi di arco (arricchimenti in LILE e LREE ed impoverimenti in Ti, Nb e P), valori $\varepsilon^{t}Sr$ positivi e $\varepsilon^{t}Nd$ negativi che suggeriscono una derivazione da una sorgente di mantello arricchita, probabilmente, da precedenti eventi di subduzione.

Differenze nella composizione isotopica di Sr e Nd, in accordo con i dati mineralogici e geochimici, evidenziano la presenza di due gruppi distinti di dicchi felsici (il gruppo delle rioliti peralluminose (PR) e quello delle rioliti da metalluminose a debolmente peralluminose (MmPR)). È proposto che i filoni leucocratici peralluminosi siano derivati per processi di fusione parziale da sorgenti crostali metasedimentarie. Gli alti rapporti $(^{87}Sr/^{86}Sr)_t$ (0,7154 ÷ 0,7173) e i valori negativi di $\varepsilon^{t}Nd$ (–7,4) di questo gruppo sono confrontabili con quelli delle litologie metasedimentarie del basamento ercinico sardo. I bilanci di massa effettuati indicano che solamente i filoni riolitici MmPR a più basso contenuto di SiO_2 potrebbero derivare dalle rocce filoniane basico-intermedie per processi di cristallizzazione frazionata. Al contrario, appare verosimile che la maggior parte dei filoni riolitici del gruppo MmPR derivi da magmi generatisi dalla fusione parziale di sorgenti crostali. I relativamente bassi rapporti $(^{87}Sr/^{86}Sr)_t$ e alti valori $\varepsilon^{t}Nd$ (rispettivamente, 0,7076 ÷ 0,7089 e –5,7 ÷ –6,3) che caratterizzano questo gruppo di filoni felsici, simili a quelli riscontrati tra le rocce filoniane basiche e intermedie, richiede una sorgente con una composizione isotopica di Sr e Nd meno evoluta di quelle riscontrate per il basamento metamorfico sardo e presuppone il coinvolgimento di una componente di mantello nelle sorgenti crostali dei filoni leucocrati da metalluminosi a debolmente peralluminosi.

KEY WORDS: *Sardinia, Late-Hercynian dykes, Rb-Sr mica ages, Sr-Nd isotopes*

INTRODUCTION

Late-Hercynian dyke swarms crosscut, along preferred directions, the granitoids of the Sardinia-Corsica Batholith, the metamorphic basement and the late-Hercynian volcanics.

The first detailed investigations on this magmatism (Atzori and Traversa, 1986; Vaccaro, 1990, Traversa and Vaccaro, 1992) pointed out that in Sardinia the hypabyssal activity occurred during two main phases, one preceding, the other following, the Permian volcanism. The products of the former phase are distributed all over the island and consist of medium and high-K calc-alkaline basic and intermediate rocks (prevalently basaltic andesites and andesites), associated with metaluminous and peraluminous dykes, rhyolitic in composition (granitic porphyries, aplites, and microgranites). Rb-Sr and ^{40}Ar-^{39}Ar mineral ages (Vaccaro *et al.*, 1991) for the dykes of the first stage, clustering around 300-290 Ma and 270 Ma, suggest two different periods of activity during the late-Carboniferous and the lower Permian.

The following stage consists of prevalently basaltic and rare felsic dykes. Among the former ones, transitional types (Ol-Hy normative, assuming Fe_2O_3/FeO ratio = 0.15) prevail spreading all over the central and northern area of Sardinia. In the southern sector of the island, Qz-normative subalkaline basalts are present, while alkaline basic rocks were found almost exclusively in a narrow area near the Posada shear zone, in northern Sardinia (Traversa *et al.*, 1991; Traversa *et al.*, 1997). The emplacement age of this «basaltic phase» is poorly defined. However, field and geochronological evidence suggests a late-Permian age. K-Ar and ^{40}Ar-^{39}Ar dating on the alkaline dyke suite yielded ages around 240÷230 Ma (Baldelli *et al.*, 1986; Vaccaro *et al.*, 1991). Transitional types too, although geochronological data are not available, are supposed to belong to the late Permian phase. Actually, they are associated with alkaline dykes in uncrossing en echelon structures (Traversa *et al.*, 1991) and crosscut the Permian volcanics (Traversa, 1969), whose published oldest age in northern Sardinia was 267 ± 7 Ma (Edel *et al.*, 1981). Nevertheless, the Rb-Sr ages of 288 ± 11 Ma, obtained on rhyolites from the Autunian volcano-sedimentary sequences of Gallura (northern Sardinia), (Novi, 1995; Del Moro *et al.*, 1996) could age the lower limit of Permian volcanism and, consequently, dykes intruding volcanics. In this scenario, at least in northern Sardinia, most of the late-Hercynian hypabyssal products, including the calc-alkaline ones at 270 Ma, should be considered as following the Permian volcanism.

Late-Hercynian dyke magmatism of southern Corsica is similar to that of Gallura as concerns geochemical characters as well as the NE-SW prevailing trend of dykes (Pasquali and Traversa, 1996; Pasquali, 1998).

In the Sarrabus area (SE Sardinia) (fig. 1), the Paleozoic basement is injected by impressive swarms of mafic and felsic dykes (Brotzu and Morbidelli, 1974; Pirinu, 1991; Ronca, 1996; Ronca and Traversa, 1996). The petrographic, mineralogical and chemical characterization of the Sarrabus dyke activity is given in Ronca and Traversa (1996).

In this paper, Rb-Sr muscovite and biotite ages on several groups of dykes from Sarrabus are presented to better constrain the age of dyke magmatism. Moreover, Sr and Nd isotopic data are reported with the aim of investigating sources of magmas as well as the processes that contributed to their evolution. In order to examine crystal fractionation as the possible evolutionary mechanism, major-element least squares fractionation models and Rayleigh fractionation models are tested. In addition, the effect of crustal assimilation, associated with fractional crystallization is also examined.

GEOLOGICAL SETTING AND FIELD DATA

The crystalline Paleozoic basement of SE Sardinia is dominated by the Sarrabus granitoid massif, mainly composed of granodiorites, monzogranites and leucogranites (Brotzu and Morbidelli, 1974; Brotzu *et al.*, 1983). Basic septa and a stratified gabbroic complex occur enclosed in the southernmost part of the massif (Tommasini, 1993). Besides, in the southern sector, close to the town of Villasimius, little stocks and veins of albite-rich monzonitic to syenitic rocks are present (Brotzu *et al.*, 1978; Pirinu, 1991; Pirinu *et al.*, 1996). In the northern edge of the massif, near Burcei village, a tonalitic-leucogabbronoritic intrusive complex occurs (Tommasini, 1993; Brotzu *et al.*, 1993). The plutons emplaced during the post-collisional phase of uplift and extension, successive to the Variscan compressive events.

Dykes especially crosscut the late-Carboniferous granitoids of the Sarrabus Massif while they are less widespread northward, at the border with the Gerrei region, where they intrude the metamorphic basement. No dyke is affected by the Hercynian metamorphic events. On the basis of such field evidence, dykes have been generally referred to a post-tectonic late Carboniferous to upper Permian magmatism. The time-span during

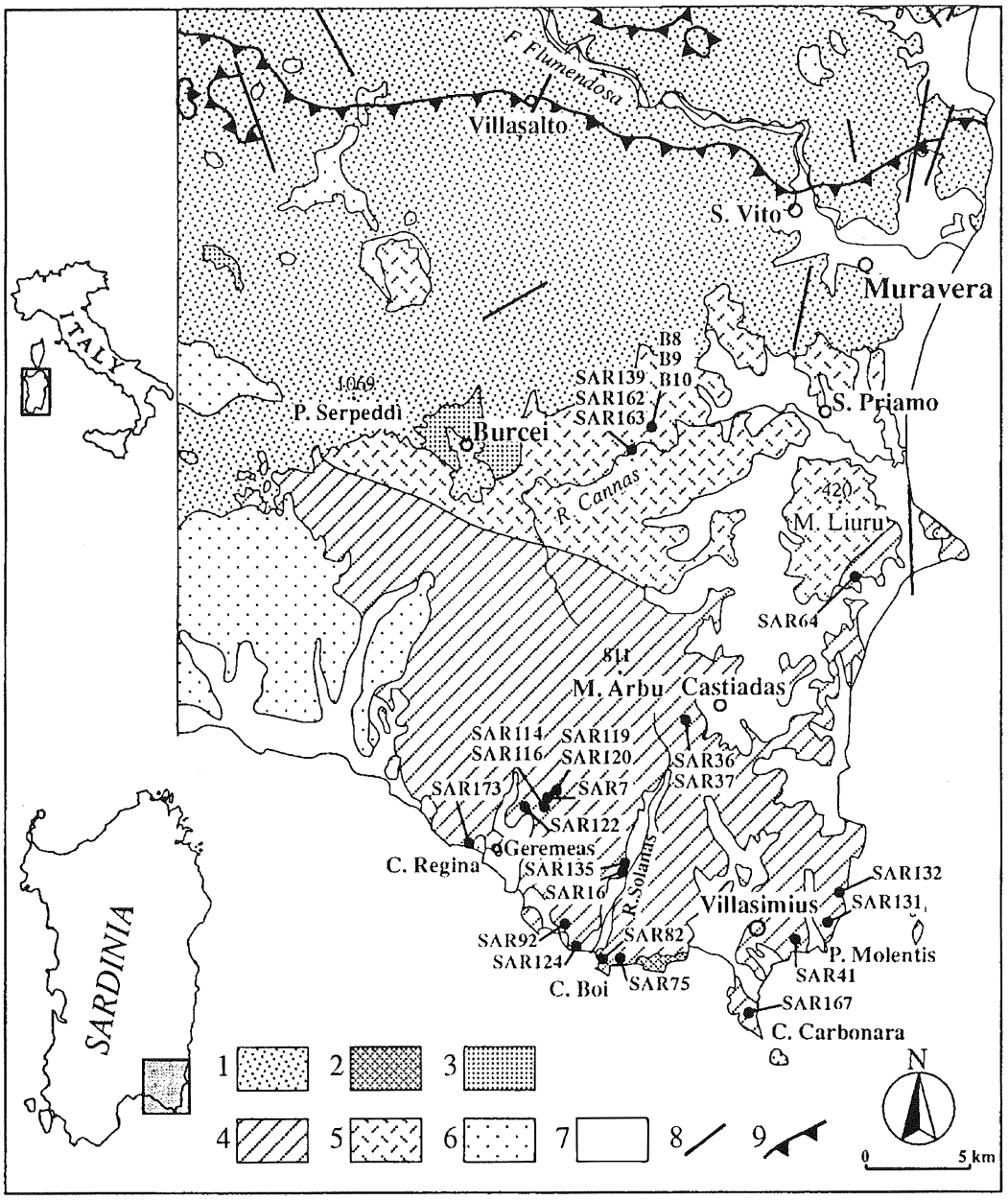

Fig. 1 - Geological sketch map of the Sarrabus area (modified after Carmignani *et al.*, 1987) showing the location of samples analysed for isotope composition. 1) Metamorphic basement – Genn'Argiolas and Gerrei Units - Metasediments and metavolcanics (Cambrian p.p. – Lower Carboniferous). 2) Hercynian Batholith – Gabbroic complex. 3) Hercynian Batholith – Burcei gabbrotonalitic body. 4) Hercynian Batholith – Monzogranites and granodiorites. 5) Hercynian Batholith – Biotite leucogranites. 6) Mesozoic-Cenozoic sediments. 7) Continental and beach deposits (Pliocene-Quaternary). 8) Faults. 9) Contact between tectonic units derived from different paleogeographic domains.

which the granitoids of the Sarrabus massif emplaced (311-295 Ma; Nicoletti *et al.*, 1982; Pirinu, 1991; Brotzu *et al.*, 1993) pre-dates the dyke activity in the studied area.

Dyke swarms intruded the basement prevalently along N140°-160°E and N-S trends. Taking into account the late-Hercynian stress pattern, as proposed for southern Sardinia by Arthaud and Matte (1975; 1977a; 1977b), such main trends appear parallel to the maximum compression direction (σ_1) and to a left side fault system, respectively (Ronca, 1996; Ronca and Traversa, 1996).

Field geology enabled us to recognize in the hypabyssal activity of Sarrabus three groups of dykes, different for structural, textural and compositional characters and to outline a sequence of intrusion events:

FD_1) 10-30 cm thick, fine- to medium-grained, generally two-mica leucogranite dykes and up to 2m thick, aplitic-micropegmatitic leucogranite dykes with muscovite-rich pegmatite pockets. These intrusions may appear both as irregular wavy ribbons and as strongly dipping dykes with planar walls. Steadily crosscut by following groups of dykes, they seem to represent the earliest phase of hypabyssal activity.

FD_2) Very thick (10-30 m) dykes of biotite or biotite-muscovite porphyries, microgranites and aplites. They often crosscut the dykes of the first phase and are frequently intruded by the dykes of the third phase.

MD) Variably thick (0.5-10 m), usually fine-grained mafic dykes. They are preferentially arranged in en-echelon intrusion sets but it is not rare to observe mutual intersections. These intrusions, crosscutting all other groups of dykes, seem to represent the final stage of the hypabyssal magmatism.

PETROGRAPHY

Dyke rocks usually show a fine grain that makes an accurate modal classification difficult. Therefore, in the present study, as in the previous papers on Sardinia dyke magmatism (Traversa *et al.*, 1997 and references therein), a classification based on whole-rock chemistry is employed. CIPW norm (calculated assuming Fe_2O_3/FeO ratio = 0.15, with the exception of the felsic samples for which Fe_2O_3/FeO is left unchanged), mineral chemistry and rock texture are also taken into account. Further, the nomenclature of volcanics is generally adopted, although for some microgranular rocks, names such as microgabbros, microdiorites, microtonalites and microgranites should be more suitable.

The Sarrabus dyke products define a subalkaline association composed of basic-intermediate calc-alkaline rocks and of granite porphyries, aplites and microgranites mainly rhyolitic in composition. The calc-alkaline sequence includes dominant basaltic andesites and andesites, a smaller volume of basalts (CaB) and extremely rare dacites; thus, the association tends to assume a bimodal distribution (fig. 2). A small group of tholeiitic basalt dykes (ThB) that were supposed to be

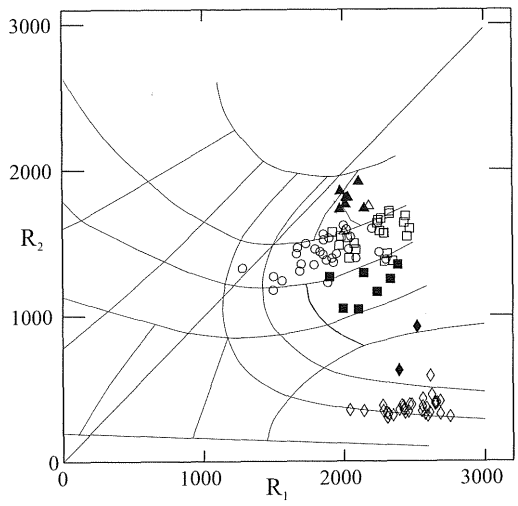

Fig. 2 – Distribution of the Sarrabus dyke rocks in the R_1-R_2 diagram (after De La Roche *et al.*, 1980; R_1 = 4Si-11(Na+K)-2(Fe+Ti), R_2 = 6Ca +2Mg +Al). Symbols: ▲ tholeiitic dykes (ThB); △ calc-alkaline basaltic dykes (CaB); □ medium-K basaltic andesitic dykes; ○ medium/high-K basaltic andesitic dykes; ■ medium/high-K andesitic dykes; ◆ dacitic dykes; ◇ rhyolitic dykes.

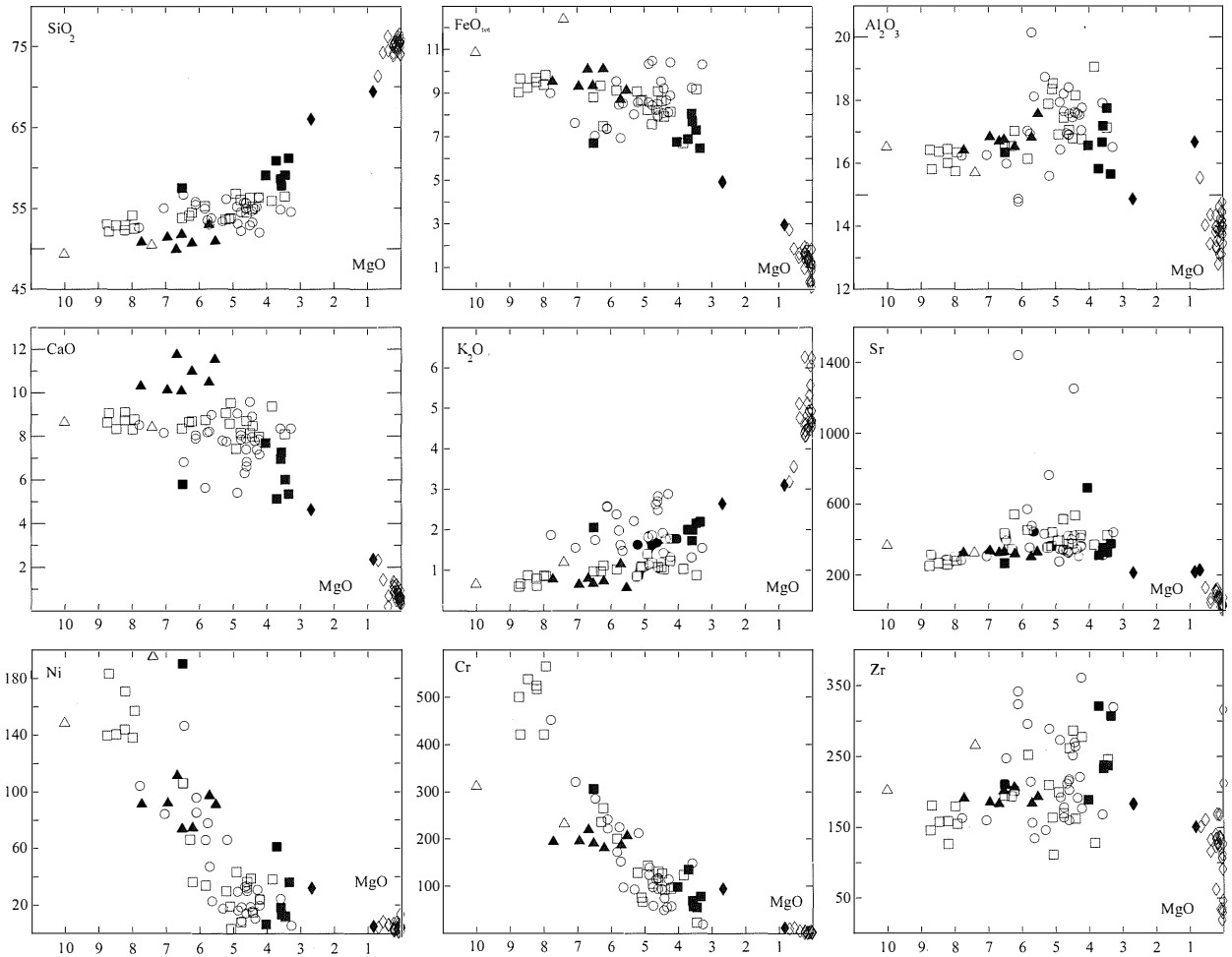

Fig. 3 – SiO_2, FeO_{tot}, Al_2O_3, CaO, K_2O, Sr, Ni, Cr and Zr *vs* MgO diagrams for the studied rocks. Major oxides are espressed in wt% (calculated dry), trace elements in ppm. Symbols as in fig. 2.

related to the late-Permian hypabyssal activity (Traversa and Vaccaro, 1992), are also present (Ronca and Traversa, 1996).

Among the felsic dykes, the aplitic-microgranitic to micropegmatitic rocks of the FD_1 group are made up of plagioclase (An_{17-2}), perthitic orthoclase or microcline (Or_{85-97}), minor amounts of biotite, almost always primary muscovite and, occasionally, spessartine-rich garnet. Tourmaline, apatite, zircon, monazite, rutile and magnetite are common accessories.

The thick dykes of group FD_2 are mainly represented by porphyritic types consisting of plagioclase (An_{37-16}), biotite, perthitic alkali-feldspar and quartz phenocrysts. The fine-grained groundmass is made up of oligoclase-albite plagioclase, alkali-feldspar, quartz and often chloritized biotite. Primary muscovite may occur as minute crystals in the groundmass. Accessories include garnet, allanite, zircon, monazite, rutile, ilmenite and magnetite.

Petrography and mineralogy of calc-alkaline basalts, basaltic andesites and andesites are very similar. Textures are variably porphyritic or glomeroporphyritic, seriate, or aphyric microgranular. Pargasite to ferro-edenite is the dominant mafic mineral. Augite is frequently found as relict enclosed in the amphibole crystals and it becomes the dominant mafic phase only in few high-Mg basaltic andesites. Olivine occurs as wholly altered phenocrysts; small amounts of interstitial biotite are present. Plagioclase is found as phenocryst (An_{86-74}) and in the groundmass (An_{66-23}). Interstitial alkali-feldspars at times occur only in the groundmass of high-K basaltic andesites. Ilmenite, pyrite, magnetite, titanite, apatite and allanite are the accessory phases. The very rare dacitic dykes (2 out of 96 analysed samples) show contrasting petrographic features, as the mineralogical assemblage is similar to that of the andesites in one case and to that of the rhyolites in the other one.

The tholeiitic basalts show phenocrysts of plagioclase (An_{69-46}), augite and olivine, the last one completely replaced by a talc, carbonate and chalcedony aggregate. The fine- to medium grained, ophitic sub-ophitic groundmass is made up of labradorite (An_{70-50}), augite, magnetite and rare interstitial biotite. Xenocrysts of reverse zoned plagioclase (An_{46-56}) and quartz with augite coronas are rarely present.

MAJOR AND TRACE ELEMENT GEOCHEMISTRY

Representative compositions of the analysed Sarrabus dykes are reported in Table 1 while a larger set of analyses is in Ronca (1996). Sarrabus mafic and intermediate dykes are metaluminous, have SiO_2 ranging from 49.2 to 65.9 wt% (H_2O-free) and show a variable alkali content ($Na_2O + K_2O$ 2.4 ÷ 6.3 wt%). The calc-alkaline basic and intermediate rocks display a continuous variation of the K_2O content from medium-K to high-K types (Peccerillo and Taylor, 1976). For simplifying purposes, in the figures and table only two groups of basaltic andesites are distinguished. A clearly medium-K group that also comprises the least differentiated *cpx*-dominant basaltic andesites and the medium/high-K one consisting of amphibole-dominant basaltic andesites.

Although calc-alkaline rocks show wide major and trace element variations, some correlation trends can be observed (fig. 3; see also Ronca and Traversa 1996 fig. 13-14). Generally, with decreasing MgO, SiO_2, Na_2O and K_2O increase, while, CaO and Al_2O_3 and, in some cases, FeO_{tot} remain constant up to MgO = 7 ÷ 6.5 wt% and then decrease. For some of the least evolved mafic rocks, negative correlation between TiO_2 and MgO can be observed. With decreasing MgO, Rb, Ba, Zr, La and Ce variably increase, Ni and Cr decrease, Sr tends to increase and just for MgO lower than 4.5 wt% decreases. The group of the cpx dominant medium-K basaltic andesites (high-Mg BA) displays high values of Ni, Cr (138 ÷ 183 ppm, 421 ÷ 565 ppm, respectively) and MgO (7.9 ÷ 8.7 wt% calculated dry). Ni and Cr contents are similar or higher than those of the calc-alkaline basalts.

TABLE 1

Whole-rock major (wt %) and trace element (p.p.m.) analyses for selected samples of dyke rocks from Sarrabus.

	Tholeiitic basalts						Calc-alk. basalts		Medium-K basaltic andesites						Medium/high-K basaltic andesites		
	B8[1]	B10[1]	B9[1]	SAR162	SAR163	B7[1]	SAR41	SAR75	SAR64	SAR15	SAR36	SAR40	SAR37	SAR89	SAR82	SAR135	SAR124
SiO_2	46.61	48.16	48.23	49.30	49.53	50.01	47.29	48.63	50.71	51.21	52.57	53.01	53.41	55.48	50.28	50.97	53.32
TiO_2	1.40	1.51	1.56	1.38	1.49	1.28	1.29	1.65	0.97	0.87	1.32	0.97	1.22	1.20	1.53	1.51	1.36
Al_2O_3	15.58	15.56	15.68	16.13	16.03	15.88	15.80	15.13	15.67	15.46	16.07	16.56	15.60	16.50	15.55	16.82	17.19
Fe_2O_3	4.17	3.16	3.15	4.33	3.70	3.50	3.57	4.77	3.17	3.31	2.82	2.55	3.72	2.96	3.99	3.37	2.61
FeO	5.65	6.19	6.76	5.01	5.61	5.06	7.18	7.65	5.78	6.21	6.54	4.99	5.46	5.35	6.18	5.79	5.54
MnO	0.23	0.18	0.21	0.18	0.17	0.16	0.19	0.21	0.16	0.20	0.17	0.16	0.17	0.16	0.18	0.17	0.11
MgO	6.23	7.33	5.90	6.66	6.25	5.39	9.58	7.13	8.34	7.93	6.12	6.05	5.63	4.79	4.60	4.23	4.33
CaO	10.98	9.78	10.41	9.72	9.63	9.88	8.29	8.10	8.25	8.80	8.41	8.46	8.45	7.25	8.57	8.53	7.78
Na_2O	1.86	2.30	2.32	2.60	2.73	2.21	1.67	1.86	1.82	2.09	2.16	3.31	1.91	2.48	2.78	2.85	2.95
K_2O	0.75	0.74	0.70	0.62	0.65	1.09	0.63	1.15	0.58	0.60	0.95	1.09	0.99	1.38	1.09	1.37	1.88
P_2O5	0.29	0.26	0.32	0.31	0.30	0.29	0.50	0.55	0.27	0.26	0.34	0.42	0.44	0.32	0.30	0.41	0.73
L.O.I.	6.24	4.43	4.75	3.76	3.90	5.24	3.99	3.18	4.26	3.07	2.53	2.44	3.01	2.13	4.95	3.98	2.20
V	186	195	203	193	202	160	166	186	174	175	172	150	200	182	238	231	170
Cr	220	193	181	195	191	187	311	232	500	518	236	265	201	144	140	75	50
Co	—	—	—	77	64	—	58	42	46	43	44	37	38	34	34	25	17
Ni	111	91	74	92	73	97	149	195	140	171	66	36	34	43	16	15	16
Cu	—	—	—	21	38	—	21	33	38	27	21	24	12	13	19	31	21
Zn	—	—	—	137	126	—	118	119	95	88	119	74	126	103	105	107	58
Rb	104	44	75	45	29	51	26	48	23	27	26	46	29	39	48	67	51
Sr	326	324	319	336	332	304	365	322	252	259	344	540	456	391	339	418	1250
Y	36	31.0	36.4	27.3	29.2	29	29.0	35.1	22.7	19.9	27.1	23.9	29	26.3	30.6	32.7	31.4
Zr	183	191	206	185	201	184	202	265	146	126	193	201	252	199	192	264	270
Nb	9	8	9	7	8	9	15	16	n.d.	n.d.	12	13	14	13	10	16	21
Ba	207	230	227	280	288	269	261	440	259	234	414	337	460	537	552	524	1694
Pb	—	—	—	16	12	—	12	13	12	9	13	15	8	14	14	10	5
Th	—	—	—	1	6	—	2	3	6	3	4	5	6	6	6	6	20
La	22.8	19.2	22.0	18.4	19.8	20.0	28.1	24.9	18.2	15.6	23.1	28.0	32.4	30.0	21.7	34.7	137.5
Ce	48.6	43.3	51.1	42.0	44.9	45.0	65.7	58.6	39.7	32.8	48.4	60.0	88.4	62.6	46.5	74.2	252.7
Pr	—	—	—	5.5	5.8	—	8.9	8.1	5.2	4.2	6.1	7.9	—	7.7	5.9	9.4	28.2
Nd	24.6	21.5	25.1	23.5	25.0	—	39.3	36.2	22.0	17.5	26.5	32.8	—	30.8	25.1	40.6	105.2
Sm	6.4	5.3	6.1	5.2	5.3	—	7.6	7.7	4.8	3.7	5.6	6.8	—	6.7	5.8	8.2	16.6
Eu	1.5	1.4	1.7	1.6	1.6	—	1.8	2.2	1.2	1.1	1.6	1.7	—	1.6	1.6	2.0	3.7
Gd	5.3	4.6	5.3	4.8	5.2	—	6.1	6.6	4.4	3.4	4.9	5.5	—	5.3	5.0	7.0	11.4
Tb	—	—	—	0.8	0.8	—	0.9	1.1	0.7	0.6	0.8	0.9	—	0.8	0.9	1.1	1.3
Dy	5.2	4.5	5.1	4.7	5.2	—	5.4	6.2	3.9	3.3	4.7	4.7	—	4.6	5.2	6.1	6.3
Ho	—	—	—	1.0	1.1	—	1.1	1.3	0.8	0.8	1.0	1.0	—	1.0	1.2	1.3	1.2
Er	2.8	2.5	2.9	2.7	2.9	—	2.8	3.3	2.1	1.9	2.6	2.3	—	2.3	2.9	3.1	2.9
Tm	—	—	—	0.4	0.4	—	0.4	0.5	0.3	0.3	0.4	0.3	—	0.4	0.4	0.4	0.4
Yb	2.6	2.3	2.7	2.6	2.9	—	2.6	3.3	2.1	2.0	2.7	2.2	—	2.3	3.1	3.0	2.6
Lu	0.4	0.4	0.5	0.5	0.5	—	0.4	0.5	0.3	0.3	0.4	0.3	—	0.4	0.5	0.5	0.4
$(La/Yb)_n$	5.89	5.69	5.56	4.72	4.61	—	7.30	5.15	5.83	5.33	5.84	8.49	—	8.65	4.80	7.85	36.21
Mg_v*	57.3	62.13	55.43	60.19	58.57	57.04	65.09	54.7	66.14	63.57	57.69	62.68	56.38	54.73	48.77	49.23	52.61
ASI	0.67	0.72	0.69	0.74	0.73	0.72	0.91	0.85	0.87	0.79	0.84	0.79	0.84	0.92	0.75	0.81	0.89

—, not determined. n.d., not detected. $Mg_v^* = Mg/Mg+Fe^{2+}$ assuming Fe_2O_3/FeO ratio = 0.15. ASI = Al_2O_3/Na_2O+K_2O+CaO molar ratio corrected for CaO content of apatite. [1] Major and trace element data from Atzori and Traversa (1986), REE data from Traversa and Vaccaro, (1992).

TABLE 1, *continued*

	Medium/high-K bas. andesites and andesite				Dacites		Rhyolites (MmPR)					Rhyolites (PR)				
	SAR119	SAR92	SAR50	SAR7	SAR16	SAR131	SAR31	SAR87	SAR132	SAR139	SAR13	SAR25	SAR116	SAR173	SAR120	SAR114
SiO_2	53.81	54.65	55.00	56.95	64.45	70.41	73.26	73.38	73.42	75.06	75.16	73.41	74.62	74.83	75.19	75.53
TiO_2	0.99	1.20	1.16	1.25	0.69	0.31	0.12	0.24	0.17	0.11	0.04	0.11	0.03	0.01	0.04	0.05
Al_2O_3	17.76	14.48	15.50	16.21	14.50	15.33	13.87	13.88	13.83	13.45	14.12	14.44	14.37	14.34	14.16	14.05
Fe_2O_3	2.35	2.75	2.89	3.02	1.95	1.02	1.16	0.85	1.37	0.88	0.26	1.22	0.29	0.44	0.23	0.23
FeO	5.53	4.73	4.24	5.11	3.08	1.77	0.76	1.07	0.69	0.51	0.09	0.28	0.15	0.85	0.11	0.04
MnO	0.14	0.13	0.14	0.14	0.10	0.07	0.05	0.05	0.07	0.04	0.02	0.04	0.02	0.06	0.03	0.02
MgO	4.45	5.98	6.27	3.48	2.61	0.68	0.02	0.54	0.23	0.19	0.04	0.12	0.06	0.03	0.09	0.05
CaO	7.63	7.73	6.62	6.75	4.55	2.28	0.63	1.41	1.32	1.10	0.93	0.88	0.58	0.36	0.54	0.39
Na_2O	2.23	2.89	3.32	2.47	3.02	3.64	4.55	3.98	3.48	3.74	4.24	3.88	3.54	3.66	3.46	2.69
K_2O	1.62	2.51	1.68	1.70	2.59	3.14	4.65	3.52	4.54	4.29	4.66	4.43	5.53	4.67	5.28	6.00
P_2O5	0.26	1.15	0.43	0.35	0.24	0.10	0.01	0.06	0.05	0.04	0.01	0.03	0.16	0.04	0.18	0.22
L.O.I.	3.23	1.80	2.75	2.58	2.21	1.25	0.92	1.03	0.83	0.59	0.44	1.16	0.64	0.72	0.69	0.74
V	156	144	146	172	103	24	n.d.	20	n.d.	n.d.	11	n.d.	n.d.	n.d.	n.d.	n.d.
Cr	94	242	285	69	95	10	n.d.	12	5	n.d.	2	n.d.	n.d.	0	n.d.	6
Co	25	34	39	34	34	5	37	32	2	1	35	33	2	3	2	4
Ni	14	96	147	19	32	4	5	8	7	4	4	3	6	14	5	4
Cu	14	15	95	34	19	4	3	5	3	5	5	3	1	12	2	n.d.
Zn	93	94	95	104	66	49	64	33	43	33	14	30	14	26	17	14
Rb	71	53	63	59	90	103	162	89	160	135	141	167	199	293	239	217
Sr	418	1444	395	342	212	227	73	129	115	122	19	97	32	2	21	20
Y	23	27.0	22.6	26.6	22.2	26.9	50.6	24.6	20.3	23.0	25.6	23.3	34	56	28	4.7
Zr	160	341	246	233	182	151	316	161	134	127	34	125	32	46	35	19
Nb	9	27	13	15	13	11	22	11	11	12	5	12	8	14	15	7
Ba	410	2210	304	610	604	714	1025	1000	719	672	71	747	93	18	42	38
Pb	7	13	13	15	22	23	27	20	31	32	44	31	50	32	45	42
Th	6	31	10	6	12	14	19	22	20	26	15	18	9	14	5	6
La	23.9	169.1	38.2	36.4	30.9	36.4	69.7	43.0	43.4	42.2	4.1	38.3	5.9	8.2	8.5	1.4
Ce	26.7	312.4	76.4	75.9	61.7	69.3	135.3	84.1	81.2	78.4	13.1	75.3	n.d.	7.0	n.d.	2.4
Pr	—	35.4	9.2	9.1	7.3	8.0	16.5	8.7	8.7	8.6	1.3	8.2	—	—	—	0.3
Nd	—	129.0	35.9	36.6	28.2	29.4	64.5	29.5	30.0	30.3	5.6	28.2	—	—	—	0.9
Sm	—	18.2	6.5	7.6	5.6	6.0	11.9	5.5	5.1	5.5	2.1	5.3	—	—	—	0.3
Eu	—	3.8	1.7	1.7	1.2	1.0	1.7	0.8	0.7	0.7	0.2	0.7	—	—	—	0.1
Gd	—	12.1	5.0	6.0	4.5	4.9	9.8	4.4	4.1	4.3	2.3	4.2	—	—	—	0.4
Tb	—	1.3	0.7	0.9	0.7	0.8	1.5	0.7	0.6	0.7	0.5	0.7	—	—	—	0.1
Dy	—	6.1	4.2	4.8	3.9	4.7	8.7	4.1	3.7	4.0	3.9	3.8	—	—	—	0.8
Ho	—	1.1	0.9	1.0	0.8	1.0	2.0	0.9	0.7	0.8	0.9	0.9	—	—	—	0.2
Er	—	2.4	2.2	2.5	2.1	2.5	5.3	2.7	1.9	2.1	2.6	2.3	—	—	—	0.4
Tm	—	0.3	0.3	0.4	0.3	0.4	0.8	0.4	0.3	0.3	0.5	0.3	—	—	—	0.1
Yb	—	2.1	2.1	2.3	2.1	2.4	5.3	2.6	2.0	2.3	3.3	2.5	—	—	—	0.5
Lu	—	0.3	0.3	0.4	0.3	0.4	0.8	0.5	0.3	0.4	0.6	0.4	—	—	—	0.1
$(La/Yb)_n$	—	54.29	12.14	10.68	10.02	10.30	8.95	10.98	14.40	12.25	0.85	10.16	—	—	—	1.83
Mg_v*	54.07	62.67	64.96	47.34	52.19											
ASI	0.95	0.77	0.85	0.94	0.94	1.15	1.02	1.09	1.07	1.06	1.03	1.14	1.15	1.23	1.18	1.2

Tholeiitic basaltic dykes have Ni (74÷111 ppm) and Cr (181÷220) contents and Mg-values (55÷62, Mg_v=100*Mg/(Mg + Fe^{2+}) assuming Fe_2O_3/FeO = 0.15) lower than the typical range of unfractionated mantle magmas (cp. Perfit *et al.*, 1980) suggesting possible fractionation of olivine and Cr-spinel. They display lower Ni, Cr and MgO and higher REE contents than the less evolved cpx-dominant medium-K basaltic andesites do (cp. SAR64 and SAR15 in Table 1). Moreover, major and trace element variation trends of tholeiitic basalts are discordant from those defined by the calc-alkaline dyke rocks. On this ground, the existence of fractionation links between tholeiitic basalts and the intermediate calc-alkaline types is unlikely, as also highlighted by mass balance calculations.

The chondrite-normalized REE patterns of basic and intermediate dykes display moderate

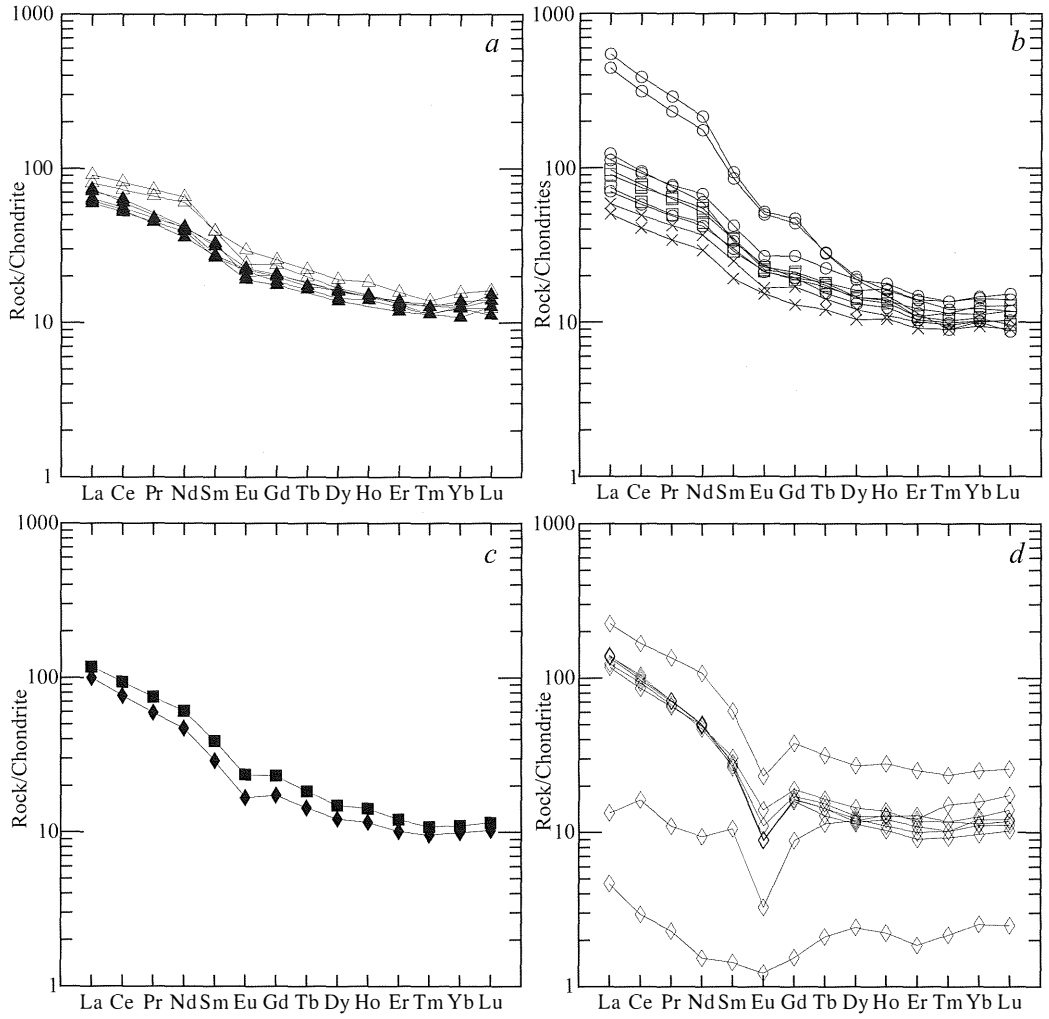

Fig. 4 – Chondrite-normalized REE patterns of selected dyke rocks from Sarrabus. Normalizing values after Boynton (1984). *a)* Tholeiitic dykes (▲) and calc-alkaline basaltic dykes (△); *b)* high-Mg medium-K basaltic andesitic dykes (×) cp.; Table 1 SAR64 and SAR15), medium-K basaltic andesitic dykes (□), medium/high-K basaltic andesitic dykes (○); *c)* medium/high-K andesitic dykes (■) and dacitic dykes (◆); *d)* rhyolitic dykes (◇).

to strong LREE/HREE fractionation (La_n/Yb_n 4.6÷54.3) with variable LREE/MREE enrichments (La_n/Sm_n 2÷5.8), slightly HREE fractionation (Tb_n/Yb_n 1.3÷2.77) and no or small negative Eu anomalies (fig. 4*a*, 4*b*, 4*c*). A general increase of the REE abundances and La_n/Yb_n ratios with increasing fractionation can be observed for the calc-alkaline products (fig. 4*a*, 4*b*). However, in comparison with calc-alkaline basaltic dykes, the high-Mg basaltic andesites display a lower REE enrichment. Some high-K basaltic andesites show high LREE contents (La 440÷550 × chondrite), pronounced REE fractionations (La_n/Yb_n 36.2÷54.3) and fractionated HREE (Tb_n/Yb_n 2.3÷2.8) (fig. 4*b*,*c*) probably due to concentration of amphibole and minor phases such as apatite.

The felsic dykes are prevalently rhyolitic in composition. The analysed rhyolitic samples have SiO_2 varying in a relatively restricted range (73.2÷76.1 wt%), except one sample which is less silicic than the others (SiO_2 = 70.4 wt%) (fig. 5). Among the rhyolites, peraluminous types prevail, with alumina saturation index (ASI = molar ratio $Al_2O_3/Na_2O + K_2O + CaO$ corrected for CaO content of apatite; see Shand, 1949; Zen, 1986) ranging from 1.02 to 1.26. The peraluminous character does not seem to be related to differentiation as ASI values do not show any systematic increase with increasing SiO_2 or decreasing CaO. Most analysed samples are mildly peraluminous (ASI < 1.1), for some of them, the slight peraluminousity can be ascribed to secondary processes. On the contrary, the rhyolitic rocks with higher ASI values than 1.1, usually, contain a significant amount of primary muscovite. Thus, on the basis of the occurrence of Al-silicates. (e.g. Al-biotite, muscovite and garnet) in the mineralogic assemblage and the ASI values higher and lower than 1.1, two different groups of felsic dykes have been distinguished: the peraluminous rhyolitic dykes (PR) and the metaluminous to mildly peraluminous rhyolitic dykes (MmPR), respectively.

Although the major element variations within the felsic dykes are not clear, some correlation can be observed. Al_2O_3, MgO, CaO, FeO_{tot} and TiO_2 are negatively correlated with SiO_2. K_2O positively correlates with SIO_2; it varies from 3.18 to 6.24 wt%, but for most rhyolites it is higher than 4 wt%. PR dykes tend to have higher P_2O_5 contents in comparison with the metaluminous ones. As regards trace elements, generally, with increasing SiO_2 and with decreasing CaO, Sr decreases and Rb increases but, for similar ranges of SiO_2 values, there are large differences in trace element abundances especially for La, Ce, Th, Zr, and Ba. PR dykes exhibit significantly lower La, Ce, Zr, Th, Ba, Sr contents and higher Rb concentrations than the MmPR dykes do.

Rhyolitic dykes display variable REE abundances and different types of chondrite-normalized patterns (fig. 4*d*). Very low REE abundances (La = 5÷45 × chondrite) and flat patterns (La_n/Yb_n = 1.8) without negative Eu anomaly seem to be peculiar of PR dykes. On the contrary, the MmPR rocks usually show higher REE abundances (La = 117÷225 × chondrite), fractionated LREE patterns (La_n/Yb_n 9÷14.4; La_n/Sm_n 3.7÷5.3), moderate negative Eu anomaly and poorly fractionated HREE. On the other hand, also some of the most leucocratic MmPR rhyolites may exhibit flat REE patterns with negative Eu anomaly and low REE contents (La = 13 × chondrite, La_n/Yb_n = 0.85). REE depleted chondrite-normalized patterns have often been attributed to REE-bearing accessory phases (e.g. monazite and zircon) fractionation in highly differentiated melts (Mittlefehldt and Miller, 1983; Yurimoto *et al.*, 1990; Zhao and Cooper, 1993). However, for the rhyolitic dykes of Sarrabus, this hypothesis seems unlikely considering that the most REE-depleted PR samples show relatively high P_2O_5 contents (0.16-0.28 wt%) also comparing with those of the REE-enriched MmPR rocks (P_2O_5 0.01-0.1 wt%). Instead, it seems possible that the REE depletion of the two mica felsic dykes could be partly attributed to crustal source composition or, more likely, to the modality of melting (retention of accessory phases in the residue).

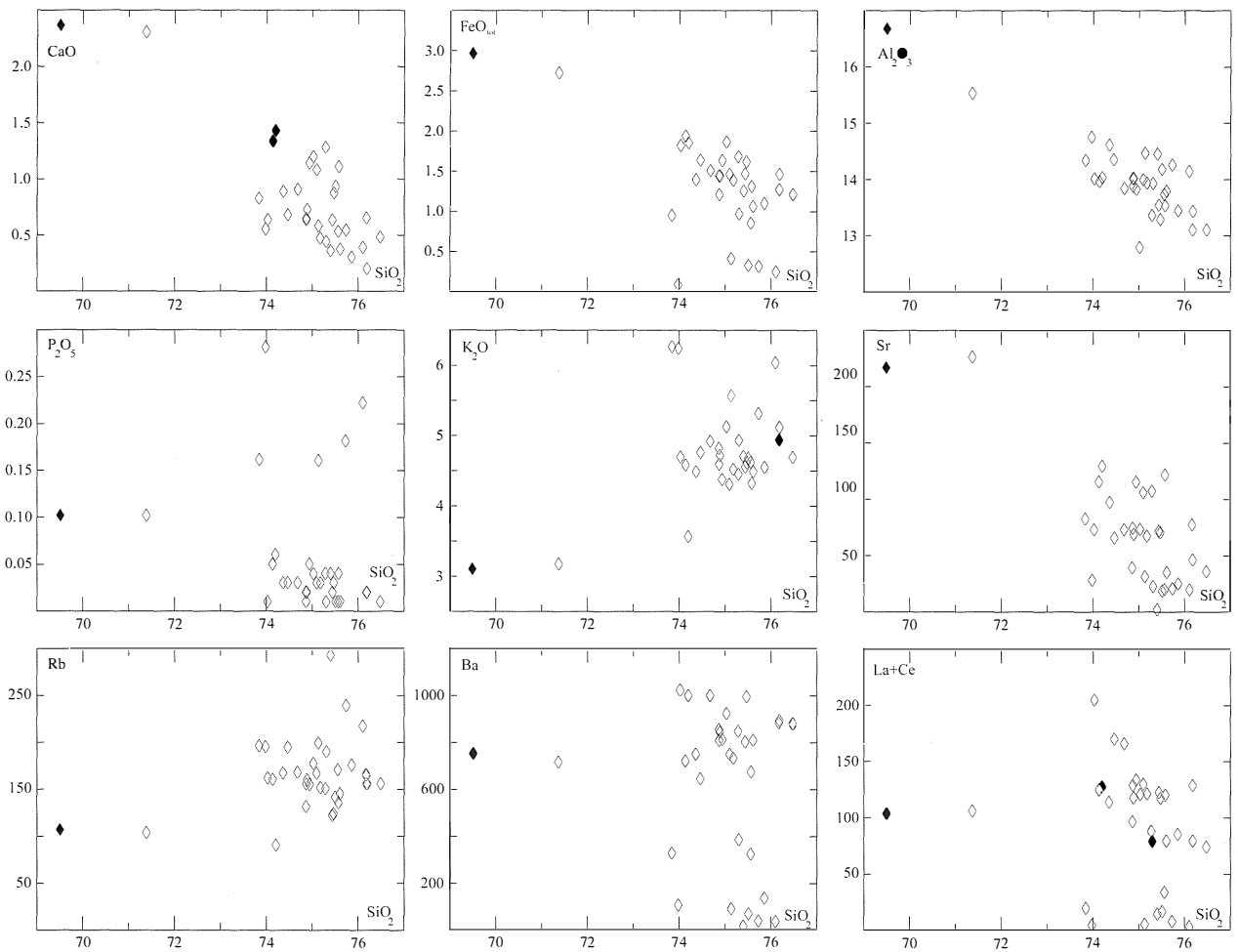

Fig. 5 - CaO, FeO_{tot}, Al_2O_3, P_2O_5, K_2O, Sr, Rb, Ba and (La+Ce) *vs* SiO_2 diagrams for the studied felsic dykes. Major oxides are espressed in wt% (calculated dry), trace elements in ppm. Symbols as in fig. 2.

Rb-Sr mica age

Four Rb-Sr muscovite ages and six Rb-Sr biotite ages were obtained on six samples from felsic and mafic dykes of Sarrabus and the analytical data are given in Table 2. A brief description of the analytical procedures is given in the Appendix.

Rb-Sr mica ages are generally interpreted as cooling ages. However, since fast cooling due to the shallow level of emplacement can be assumed for most dyke rocks, Rb-Sr mica ages can be considered to approximate emplacement ages (Hanny *et al.*, 1975; Saleeby and Sharp, 1978).

Samples SAR116, SAR114 and SAR120 are from 3 micropegmatitic PR dykes of group FD_1, all three intruding the Hercynian granitoids in the southern part of the massif. The Rb-Sr two-point (muscovite and whole-rock) isochrons yielded Rb-Sr ages of 292-293 Ma with analytical uncertainties of 3 Ma. For sample SAR116, we also obtained a 253 ± 3 Ma Rb-Sr biotite age.

Sample SAR173, from a muscovite-garnet microgranite PR dyke crosscutting the southern

TABLE 2

Rb-Sr mica ages on the Sarrabus dykes.

Sample	Material	Rb (ppm)	Sr (ppm)	$^{87}Rb/^{86}Sr$	$^{87}Sr/^{86}Sr \pm 2\sigma$	Age (Ma±2σ)
Peraluminous rhyolitic dykes (PR)						
SAR116	WR	194	30.3	18.6	0.79223±5	
	Mu	746	2.75	1155	5.5140±5	292±3
	Bt	376	12.9	87.1	1.03863±5	253±3
SAR114	WR	213	19.8	31.6	0.84769±3	
	Mu	817	2.88	1238	5.8784±3	293±3
SAR120	WR	235	19.5	35.3	0.86122±3	
	Mu	1146	2.74	2405	10.7486±6	293±3
SAR173	WR	303	2.44	421	2.47029±7	
	Mu	1047	1.39	15211	61.563±9	281±3
	Bt	2019	4.34	2737	11.354±7	270±3
Metaluminous to mildly peraluminous rhyolitic dykes (MmPR)						
SAR131	WR	102	220	1.33	0.71269±2	
	Bt	615	11.1	170	1.34709±7	264±3
SAR132	WR	155	114	3.94	0.72387±3	
	Bt	555	5.84	306	1.88394±7	270±3
SAR139	WR	134	118	3,28	0.72145±2	
	Bt	702	7.10	320	1.9254±1	267±3
Medium/high-K calc-alkaline dykes						
SAR82	WR	42.5	294	0.418	0.70858±3	
	Bt	298	19.7	44.5	0.87083±3	259±3

$\lambda^{87}Rb = 1.42 \cdot 10^{-11}$ yr^{-1}. $2\sigma = 2\sigma$ of the mean ($2\sigma/\sqrt{n}$). WR, whole rock; Mu, muscovite; Bt, biotite.

part of the Sarrabus granitoid massif near Cala Regina, gave a Rb-Sr muscovite age and a Rb-Sr biotite age of 281 ± 3 e 270 ± 3 Ma, respectively.

On three MmPR biotite-bearing porphyries, from the southeastern (Punta Molentis area: SAR131 and SAR132) and northern (Rio Cannas area: SAR139) sectors of Sarrabus Massif, three similar Rb-Sr biotite ages of 270 ±3, 264 ± 3, 267 ± 3 Ma were obtained.

A Rb-Sr biotite age of 259 ± 3 Ma was obtained on a sample (SAR82) from a basaltic andesite dyke. Unfortunately, even if biotite is often present in the groundmass of mafic dykes, it is usually scarce and often affected by chloritization, so, it was impossible to concentrate enough material for analysis from other mafic samples in order to obtain further biotite-ages.

WHOLE-ROCK SR AND ND ISOTOPIC RESULTS

Sr and Nd isotopic data on selected samples from hypabyssal products of Sarrabus are given in Table 3. Sr and Nd isotope initial ratios have been calculated taking the Rb-Sr mineral ages (Table 2) into account. Ages of 290 and 270 Ma for the rhyolitic rocks and an age of 270 Ma for the whole basic and intermediate rocks have been used to correct the isotopic ratios for decay. It must be stressed that differences of the order of 10 Ma between the assumed and effective ages do not significantly affect the calculated initial isotopic ratios in rocks having a low parent/daughter ratio. This is true for Nd isotopic data of all analysed dyke rocks and only for Sr isotopic data of basic and intermediate rocks.

Among Sarrabus dyke rocks, tholeiitic basalts display the lowest $(^{87}Sr/^{86}Sr)_t$ and the highest $(^{143}Nd/^{144}Nd)_t$ ratios, (0.70518 ± 1 ÷ 0.70532 ± 2 and 0.512215 ± 20, respectively). These data well agree with those reported by Traversa and Vaccaro (1992) ($^{87}Sr/^{86}Sr_{270}$ = 0.70515 ± 4 ÷ 0.70528 ± 2) on the same rock-types. The calc-alkaline series exhibits a large variation of the initial Sr and Nd isotopic ratios (0.70681 ± 2 ÷ 0.70968 ± 4, 0.512135 ± 20 ÷ 0.511980 ± 15, respectively), with a general increase in $(^{87}Sr/^{86}Sr)_t$ values and a decrease in $(^{143}Nd/^{144}Nd)_t$ values with fractionation. However, high-K rocks show $(^{87}Sr/^{86}Sr)_t$ values higher than those of medium-K series samples.

A wide range of the initial Sr and Nd isotopic ratios is also observed among the rhyolitic rocks (0.70757 ± 6 ÷ 0.71731 ± 130, excluding sample SAR173, and 0.512000 ± 18 ÷ 0.511885 ± 28, respectively). The highest $(^{87}Sr/^{86}Sr)_t$ and lowest $(^{143}Nd/^{144}Nd)_t$ ratios (0.71548 ± 77 ÷ 0.71731 ± 130, excluding sample SAR173, and 0.511885 ± 28, respectively) are found in the PR group. The remaining rhyolites, on the contrary, have values (0.70757 ± 6 ÷ 0.70886 ± 13 for $(^{87}Sr/^{86}Sr)_t$; 0.512000 ± 18 ÷ 0.511969 ± 19 for $(^{143}Nd/^{144}Nd_t)$ similar to those of the most evolved calc-alkaline mafic dykes. Among the PR dykes, sample SAR173 shows an $(^{87}Sr/^{86}Sr)_t$ ratio strongly sensitive to age-correction, owing to its very high $^{87}Rb/^{86}Sr$ ratio. If an age of 280 Ma is used for the age-correction, the $(^{87}Sr/^{86}Sr)_t$ ratio is equal to 0.7935 ± 0.0168. This value is rather high when compared to any potential source rock from Sardinia. On the other hand, supposing that muscovite age does not approximate the emplacement age (see discussion) and thus assuming an age of 290 Ma, the calculated $(^{87}Sr/^{86}Sr)_t$ ratio is 0.7335 ± 174 which is comparable with the isotopic compositions of the other PR dykes.

DISCUSSION

Age of the Sarrabus dyke magmatism

The whole geochronological data set obtained for Sarrabus dyke magmatism confirms the sequence of intrusion events suggested by field observations. Moreover, it is in good agreement with the radiometric ages of the plutons forming the Sarrabus granitoid massif (Brotzu *et al.*, 1993; Pirinu *et al.*, 1996

TABLE 3

Rb-Sr and Sm-Nd analytical data for whole-rock samples of Sarrabus dykes.

Sample	Rb (ppm)	Sr (ppm)	$^{87}Rb/^{86}Sr$	$^{87}Sr/^{86}Sr \pm 2\sigma$	$(^{87}Sr/^{86}Sr)_t$	ε^tSr	Sm (ppm)	Nd (ppm)	$^{147}Sm/^{144}Nd$	$^{143}Nd/^{144}Nd \pm 2\sigma$	$(^{143}Nd/^{144}Nd)_t$	ε^tNd
Hercynian Batholith granitoids from Sarrabus (assumed age 300 Ma)												
SAR167	89	339	0.762	0.71031±3	0.70706±4	41.3±0.6	5.72	30.1	0.115	0.512201±14	0.511975±21	-5.4±0.4
SAR122	146	162	2.62	0.72037±1	0.70920±11	71.7±1.6						
Peraluminous rhyolitic dykes (PR) (assumed age 290 Ma)												
SAR116	194	30.3	18.6	0.79223±5	0.71548±77	161±11						
SAR114	213	19.8	31.6	0.84769±3	0.71731±130	187±18	0.278	0.919	0.183	0.512232±14	0.511885±28	-7.4±0.5
SAR120	235	19.5	35.3	0.86122±3	0.71565±146	163±21						
SAR173	303	2.44	421	2.47029±7	0.73350±1737	417±247						
Metaluminous to mildly peraluminous rhyolitic dykes (MmPR) (assumed age 270 Ma)												
SAR131	102	220	1.33	0.71269±2	0.70757±6	48.0±0.8	5.95	29.4	0.123	0.512186±12	0.511969±19	-6.3±0.4
SAR132	155	114	3.94	0.72387±3	0.70872±15	64.3±2.2	5.11	30.0	0.103	0.512182±12	0.512000±18	-5.7±0.3
SAR139	134	118	3.28	0.72145±2	0.70886±13	66.3±1.8	5.49	30.3	0.110	0.512182±10	0.511989±17	-5.9±0.3
Medium/high-K calc-alkaline dykes (assumed age 270 Ma)												
SAR16 Dacite	91	253	1.04	0.71319±2	0.70919±4	71.1±0.6	5.63	28.2	0.121	0.512217±10	0.512003±18	-5.6±0.4
SAR7 Andesite	57	331	0.499	0.71045±5	0.70853±5	61.7±0.8	7.58	36.6	0.126	0.512191±9	0.511968±18	-6.3±0.4
SAR92 Basaltic and.	54	1305	0.119	0.71010±2	0.70964±2	77.5±0.3	18.2	129	0.085	0.512144±9	0.511994±14	-5.8±0.3
SAR124 Basaltic and.	52	1159	0.130	0.71018±4	0.70968±4	78.0±0.6	16.6	105	0.096	0.512150±9	0.511980±15	-6.1±0.3
SAR119 Basaltic and.	70	429	0.470	0.70971±3	0.70791±4	52.8±0.5						
SAR135 Basaltic and.	63	398	0.453	0.71017±2	0.70843±3	60.3±0.4	8.20	40.6	0.123	0.512262±10	0.512045±18	-4.8±0.4
SAR82 Basaltic and.	43	294	0.418	0.70858±3	0.70697±3	39.6±0.5	5.80	25.1	0.140	0.512382±9	0.512135±20	-3.0±0.4
SAR75 Basalt	47	437	0.313	0.70801±2	0.70681±2	37.2±0.3	7.66	36.2	0.128	0.512354±9	0.512128±18	-3.2±0.4
Medium-K calc-alkaline dykes (assumed age 270 Ma)												
SAR37 Basaltic and.	35	453	0.222	0.70866±4	0.70781±4	51.4±0.6						
SAR36 Basaltic and.	16	389	0.122	0.70797±3	0.70750±3	47.1±0.4	5.59	26.4	0.128	0.512273±7	0.512047±17	-4.8±0.3
SAR64 Basaltic and.	23	224	0.296	0.70836±2	0.70722±2	43.1±0.3	4.83	22.0	0.133	0.512323±11	0.512088±20	-4.0±0.4
SAR41 Basalt	33	440	0.219	0.70788±3	0.70704±3	40.5±0.4	7.61	39.3	0.118	0.512253±9	0.512044±17	-4.8±0.3
Tholeiitic dykes (assumed age 270 Ma)												
SAR162 Basalt	34	309	0.321	0.70655±1	0.70532±2	16.1±0.2	5.16	23.5	0.133	0.512450±12	0.512215±20	-1.5±0.4
SAR163 Basalt	19	302	0.178	0.70586±1	0.70518±1	14.1±0.2	5.34	25.0	0.130	0.512445±10	0.512215±19	-1.5±0.4
B10* Basalt			0.373	0.70671±1	0.70528±2	15.5±0.3						
B8* Basalt			0.881	0.70853±1	0.70515±4	13.6±0.5						
B9* Basalt			0.648	0.70773±1	0.70524±3	15.0±0.4						

Parameters used for calculation of ε^tSr and ε^tNd values: $\lambda^{87}Rb = 1.42 \cdot 10^{-11}$ yr^{-1}; $(^{87}Sr/^{86}Sr)^0_{UR} = 0.7045$ and $(^{87}Rb/^{86}Sr)^0_{UR} = 0.0816$; $\lambda^{147}Sm = 6.54 \cdot 10^{-12}$ yr^{-1}; $(^{143}Nd/^{144}Nd)^0_{CHUR} = 0.512638$ and $(^{147}Sm/^{144}Nd)^0_{CHUR} = 0.1967$ (Jacobsen and Wassemburg, 1984). *, isotopic data from Vaccaro (1990). $2\sigma = 2\sigma$ of the mean ($2\sigma/\sqrt{n}$). The uncertainties reported for initial isotopic ratios and ε^t values result from error propagation including errors for measured isotopic ratios and errors on $^{87}Rb/^{86}Sr$ and $^{147}Sm/^{144}Nd$ ratios (1% and 7%, respectively).

and references therein).

The early hypabyssal intrusions, slightly younger than the plutons that they intrude, consist of not very thick, mostly two-mica leucogranite dykes (3 Rb-Sr muscovite ages: 293-292 Ma). The quite irregular shape of these dykes, unlike the youngest ones, could suggest that the granitoid host rocks in which dykes intruded were not yet wholly solidified. The low value of the biotite age obtained from one of the PR dykes (SAR116: 253 ± 3 Ma) may be explained by an open-system behaviour due to a gradual biotite alteration, a process that is not rare in dyke rocks. Otherwise, the SAR116 Rb-Sr biotite age could be due to a reopening of the Rb-Sr system during a later local heating. For tholeiitic activity, a possible age of 250-245 Ma has been tentatively proposed (Vaccaro, 1990; Traversa and Vaccaro, 1992). However, since tholeiitic dykes occur only occasionally and far from the SAR116 outcropping area, it seems unlikely that their emplacement caused the reopening of the Rb-Sr system; moreover, we have no further similar age confirming this hypothesis.

For the muscovite-garnet microgranite dyke SAR173, there is a significant time-gap between the Rb-Sr cooling ages of the mica pair (281 ± 3 and 270 ± 3 Ma). Similar age differences (10-11 Ma) have been observed on Sardinian Hercynian plutons (Di Vincenzo *et al.*, 1994) and could be explained by a relatively slow cooling. Such hypothesis can be supported by the microgranular texture of sample SAR173. Thus for this sample, as previously supposed on the basis of Sr isotopic composition, the Rb-Sr muscovite age does not reflect the emplacement age.

The very thick porphyry, microgranite and aplite dykes emplaced later as suggested by the 3 Rb-Sr biotite ages (264 ÷ 270 Ma) obtained on MmPR dykes. However, although geochronological data clearly attesting the emplacement of PR dykes at that time are not available, field and petrographic evidence suggests a contemporaneous emplacement of both magma types.

The final stage mainly has a basic character, as shown by field relationships and by a single Rb-Sr biotite age of 259 ± 3 Ma on a mafic dyke of the calc-alkaline suite. Obviously, this age is not enough to satisfactorily define the time-span over which basic dyke activity occurred in the Sarrabus area. Furthermore, it is necessary to more accurately date the basic activity, especially the tholeiitic composition one which, for its petrochemical and isotopic signatures, has been referred to the basaltic phase following Permian volcanism (Traversa and Vaccaro, 1992; Ronca and Traversa, 1996).

Our new radiometric data integrate previous Rb-Sr and ^{39}Ar-^{40}Ar mineral ages on dyke magmatism from northern and central Sardinia, providing further information on the overall duration of the Late-Hercynian dyke magmatism in the Sardinia-Corsica area. As regards the PR rhyolitic dykes, there is no considerable difference in age between the samples from Sarrabus (Rb-Sr Ms-age: 293 ÷ 281, Rb-Sr Bt-age: 270 ± 3 Ma) and those from other sectors of Sardinia (Rb-Sr Ms-age: 298 ÷ 281, Bt-age: 291 ÷ 268 Ma; Vaccaro *et al.*, 1991). A 289 ± 9 Ma Rb-Sr biotite age (Vaccaro *et al.*, 1991) was determined on a dyke with andesitic composition from the Ogliastra region (Central Sardinia). This age, significantly older than those of other calc-alkaline dykes from northern Sardinia, led Vaccaro *et al.* (1991) to think that in central and southern Sardinia the calc-alkaline activity did not occur later than 290 Ma. On the other hand, the 259 ± 3 Ma Rb-Sr age of sample SAR82 from a basaltic andesite dyke and the field observation of calc-alkaline basic dykes crosscutting porphyries dated around 270 Ma clearly attest that, at least in the Sarrabus area, calc-alkaline hypabyssal magmatism lasted throughout the Autunian.

Geochemical and isotopic constraints on the origin of the dyke magmatism

The mafic mineralogy, the high compatible element concentrations (Ni, Cr) and the Sr and Nd isotopic composition of the least evolved rocks indicate that Sarrabus mafic dyke rocks are largely derived from a mantle source,

although fractionation occurred, as also suggested by the variable amounts of Mg-Fe mineral and plagioclase phenocrysts in the porphyritic types as well as the presence of compositionally zoned minerals (plagioclase and amphibole) in most of the mafic dykes. On the basis of petrographical, geochemical and isotopic evidence, the tholeiitic and calc-alkaline dyke groups do not appear related to each other by fractionation relationships. Compared with the less evolved calc-alkaline rocks, the higher CaO and lower MgO contents of ThB seem to indicate that ThB suffered a more conspicuous olivine fractionation from the parent magma than the calc-alkaline basalts and the high-Mg basaltic andesites did. Moreover, the overall mineralogical and geochemical data suggest that tholeiitic and calc-alkaline rocks could be derived from distinct primary mantle melts.

Basic and intermediate dykes of the calc-alkaline suite have initial $^{87}Sr/^{86}Sr$ ratios ($0.70681 \pm 2 \div 0.70919 \pm 4$) showing a positive correlation with some major (SiO_2, Na_2O, K_2O) and trace (Rb, Ba, REE) elements. As an example, fig. 6 reports the $(^{87}Sr/^{86}Sr)_t$ variation with respect to SiO_2 and MgO. Such co-variations could indicate that crustal contamination processes occurred with fractional crystallisation in the evolution of the calc-alkaline rocks. Moreover, compared with the medium-K group, the higher initial $^{87}Sr/^{86}Sr$ ratios of medium/high-K rocks suggest that the crustal contamination process variably operated within the calc-alkaline suite (the medium/high-K rocks underwent a greater amount of crustal contamination). On the other hand, Sr isotope ratios of ThB are quite constant and do not seem to correlate positively with differentiation, although small linear co-variations between $(^{87}Sr/^{86}Sr)_t$ and MgO can be observed in fig. 6*b* (inset). Moreover, as the variation ranges are not very wide, ThB having quite similar evolutionary degrees, it is difficult to assess whether such small co-variations are unsignificant or not.

Major and trace element modelling of fractional crystallisation was performed in order to check the feasibility that the above-suggested mechanisms controlled the evolution of the calc-alkaline suite. Major element mass balance calculations were carried out by least-square methods (Stormer and Nicholls, 1978) employing mineral phase compositions from EDS and EDS+WDS analyses on Sarrabus dyke rocks (Ronca, 1996; Ronca and Traversa, 1996). Only for olivine, analyses obtained on other late-Hercynian dykes from Sardinia were employed (Traversa, unpublished), since olivine was always found altered in Sarrabus samples. The removed mineral assemblages used in the calculations were based upon the mineralogy of the investigated rocks. Trace elements were tested first for fractional crystallization using the Rayleigh equation and then, in the cases for which the changeable

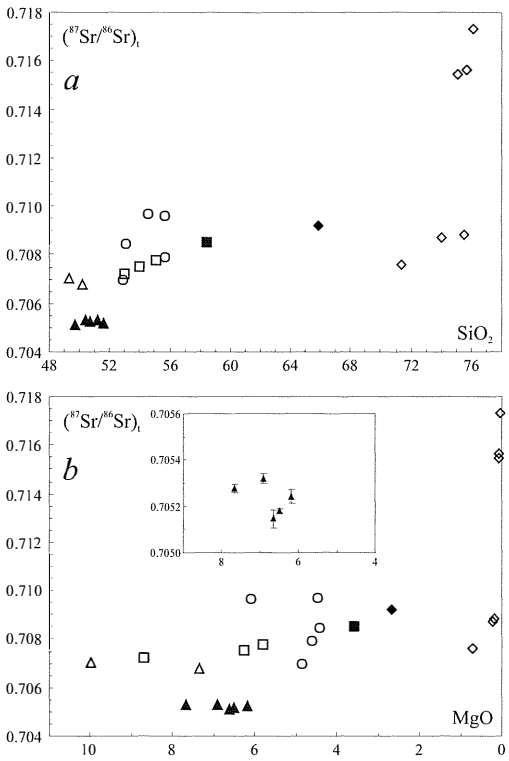

Fig. 6 – Initial Sr isotope ratio $(^{87}Sr/^{86}Sr)_t$ *vs* SiO_2 (*a*) and *vs* MgO (*b*) diagrams for selected dyke rocks from Sarrabus. Symbols as in fig. 2.

TABLE 4

Results of fractional crystallization models for the Sarrabus dyke rocks.

	from SAR41 CaB	to SAR119 BA			from SAR64 BA	to SAR7 A			from SAR7 A	to SAR131 R			to SAR87 R			to SAR139 R		
	obs	calc	obs		obs	calc	obs		obs	calc	obs		calc	obs		calc	obs	
SiO_2	49.45	55.83	55.74		53.16	58.79	58.63		58.63	71.49	71.37		74.31	74.20		75.71	75.57	
TiO_2	1.35	1.07	1.03		1.02	1.23	1.29		1.29	0.42	0.31		0.29	0.24		0.16	0.11	
Al_2O_3	16.52	18.46	18.40		16.43	16.80	16.69		16.69	15.57	15.54		14.15	14.04		13.67	13.54	
FeO_{tot}	10.86	8.01	7.91		9.05	8.28	8.06		8.06	2.79	2.73		1.98	1.85		1.47	1.31	
MnO	0.20	0.07	0.15		0.17	0.14	0.14		0.14	0.03	0.07		0.01	0.05		0.00	0.04	
MgO	10.02	4.63	4.61		8.74	3.63	3.58		3.58	0.74	0.69		0.56	0.55		0.20	0.19	
CaO	8.67	7.94	7.90		8.65	7.04	6.95		6.95	2.42	2.31		1.40	1.43		1.04	1.11	
Na_2O	1.75	2.24	2.31		1.91	2.42	2.54		2.54	3.42	3.69		3.68	4.02		3.60	3.77	
K_2O	0.66	1.38	1.68		0.61	1.26	1.75		1.75	2.97	3.18		3.33	3.56		3.81	4.32	
P_2O_5	0.52	0.37	0.27		0.28	0.42	0.36		0.36	0.14	0.10		0.27	0.06		0.33	0.04	
ΣR^2		0.14				0.36				0.17				0.26		0.44		
F (%)		53.88				59.96				54.75				48.90		46.54		
OL		38.11				29.8				7.75				6.72		7.16		
CPX		4.84				11.2				—				—		—		
AMPH		17.60				20				51.8				50.05		48.9		
PL		36.22				39.1				36.7				40.31		41.3		
ILM		1.92				—				2.4				2.40		2.47		
APA		1.31				—				1.31				0.52		0.21		
	obs	calc	obs	D	obs	calc	obs	D	obs	calc	obs	D	calc	obs	D	calc	obs	D
Rb	33	56	70	0.13	23	38	57	0.01	57	101	102	0.05	90	89	0.37	119	134	0.04
Ba	261	411	410	0.26	259	424	610	0.03	610	796	714	0.56	1015	1000	0.29	843	672	0.58
Sr	440	436	429	1.01	224	284	331	0.54	331	225	220	1.64	132	129	2.28	121	118	2.32
V	166	152	156	1.14	174	178	172	0.95	172	25	24	4.20	19	20	4.07	—	—	—
Cr	311	89	94	3.02	500	60	69	5.14	69	10	10	4.16	12	12	3.49	—	—	—
Ni	148	14	14	4.79	140	20	18	4.83	18	4	4	3.44	8	8	2.11	3	4	3.23
Zr	202	258	160	0.61	146	234	233	0.08	233	221	151	1.09	222	161	1.07	224	127	1.05
Y	29	37	23	0.59	23	29	27	0.54	27	27	27	0.97	25	25	1.08	30	23	0.87
La	28.1	35	24	0.62	18.2	30	36.4	0.05	36.4	43	36.4	0.72	50	43	0.55	54	42	0.49
Ce	65.7	80	27	0.67	39.6	64	75.9	0.07	75.9	84	69.2	0.83	99	84.1	0.63	108	78	0.54
Yb	2.6				2.1	2	2.3	0.87	2.3	2	2.4	0.92	3	2.6	0.8	2	2	1.08

Major elements were modelled using the XL-FRAC calculation program (Stormer and Nicholls, 1978). Trace element modelled values are calculated by the Rayleigh fractionation model using mineral/matrix partition coefficients from the literature. Source of data: Henderson (1986); Nielsen (1998) and references therein. CaB, calc-alkaline basalt; BA, basaltic andesite, A, andesite; R, rhyolite; calc, calculated values; obs, measured values ΣR^2, sum of the squares of the residuals; F, weight proportion of the residual liquid; OL, olivine; CPX, clinopyroxene; AMPH, amphibole; PL, plagioclase; ILM, ilmenite; APA, apatite.

isotopic data suggest crustal contamination, for assimilation + fractional crystallization using the De Paolo (1981) AFC model. The results of major element mass balance calculations and K_d values for calc-alkaline rocks from the literature (Henderson, 1986; Nielsen, 1998 and references therein) were employed as constraints. Calculations indicate that the main major element variations observed among ThB rocks (from B10 to B7; $\Sigma R^2 < 0.05$) could be produced by a 30 % fractionation of the mineral assemblage consisting of plagioclase (50.3%) + olivine (27.5%) + clinopyroxene (17.6%) ilmenite (4.6%). Nevertheless, the observed variations of most trace elements do not agree with the model. Therefore, major and trace element variations within ThB cannot be explained by fractional crystallization but they could reflect slight variations in the composition of primary parent magmas.

Crystal fractionation was investigated quantitatively on variously evolved samples of calc-alkaline suite. Among the less evolved rocks, the calc-alkaline basalt (SAR41) and, for its primitive characteristics (high Mg#, high Ni e Cr abundances), the high-Mg basaltic andesite (SAR64) have been chosen as parent magma. Major-element mass balance calculations indicate that andesitic compositions (e.g. SAR7) could be produced starting from the high-Mg basaltic andesites (e.g. SAR64) (Table 4) by removal of a mineral assemblage consisting of olivine+clinopyroxene+amphibole+plagioclase. The inferred fractionating assemblage well agrees with the petrographic data but the trace element modelling of the fractional crystallization process gives unsatisfactory results. The calculated values of the most compatible elements (Ni, Cr) agree fairly well with the observed ones. For Rb, Sr, Ba, La and Ce, on the other hand, the calculated values are lower then the measured ones, although the lowest partition coefficients for calc-alkaline basic and intermediate rocks from the literature were used. As fractional crystallization cannot account for similar trace element enrichments, also considering the increasing Sr isotopic ratios of calc-alkaline dyke samples, a combined crustal assimilation + fractional crystallization model (De Paolo, 1981) has been tested for some trace elements and the Sr isotopic ratio (Table 5). Melts of composition corresponding to that of the Hercynian calc-alkaline granitoids and of the MmPR dykes can be rejected as a contaminant because of their Sr isotopic ratios similar or lower than those of some mafic dyke samples and their high Rb contents. (cp. Table 1-2 and Tommasini *et al.*, 1995). On the other hand, a more appropriate contaminant could be found in the metasedimentary lithologies of the Sardinia basement. Sarrabus granitoid massif was intruded into the metasedimentary and metavolcanic formations of the Genn'Argiolas Unit (Carosi *et al.*, 1992 and references therein). However, as geochemical and isotopic data for the Genn'argiolas Unit are not available, we have chosen as contaminant the composition of the metasediments (metapelites and metagreywackes) of the hercynian

TABLE 5

Results of the assimilation + fractional crystallization model for the calc-alkaline mafic dykes form Sarrabus.

Contaminant		from SAR64 BA	to SAR7 A		
		obs	calc	obs	D
Rb	63	23	57	57	0.02
Ba	536	259	580	610	0.03
Sr	200	224	300	331	0.54
Zr	196	146	261	233	0.22
Y	29	23	30	27	0.65
La	36	18.2	36.6	36.4	0.18
Ce	63	39.6	75.7	75.9	0.17
Yb	2.63	2.1	2.3	2.3	0.97
$(^{87}Sr/^{86}Sr)_{270Ma}$	0.71519	0.70722	0.70852	0.70853	
F (%)			59.96		
R			0.31		

The model is calculated according to De Paolo (1981). Abbreviations as in Table 4. r = assimilation/crystallization rate. Contaminant composition from Del Moro *et al.* (unpublished) (hercyinan basement metasediments from the Giuncana area – northern Sardinia).

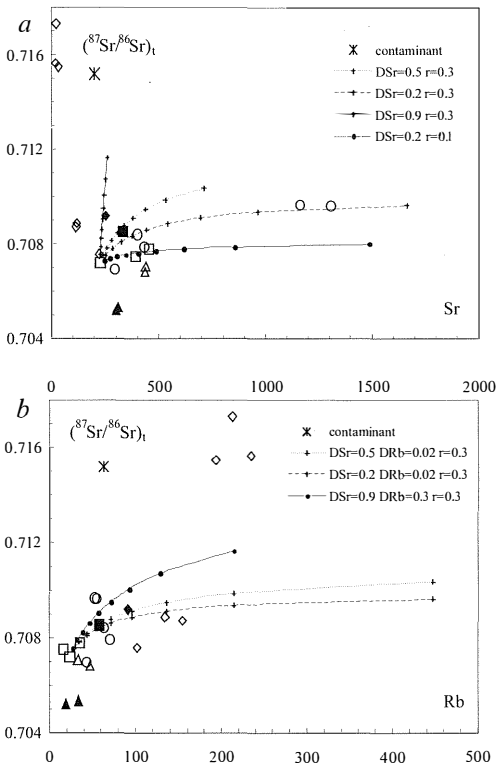

Fig. 7 - Initial Sr isotope ratio $(^{87}Sr/^{86}Sr)_t$ *vs* Sr (*a*) and *vs* Rb (*b*) diagrams for selected dyke rocks from Sarrabus. AFC trends starting from the basaltic andesite SAR64 are also shown. DSr and DRb are the bulk distribution coefficients between the fractionating assemblage and the magma for Sr and Rb, respectively. *r* = Ma/Mc assimilation/crystallization rate. Contaminant composition is reported in Table 5. Symbols as in fig. 2.

basement from the Giuncana area (northern Sardinia) (Del Moro *et al.*, unpublished data). The observed variations of some trace elements and the initial $^{87}Sr/^{86}Sr$ isotopic ratio between the high-Mg basaltic andesite SAR64 and the andesite SAR7 can be satisfactorily replicated by an AFC model, with F = 60% and *r* = 0.31 (F = weight proportion of remaining liquid; *r* = assimilation rate/ fractional crystallization rate) (Table 5, fig. 7). Some slight discrepancies for Sr, Ba and Zr suggest that a contaminant having higher Sr and Ba contents and lower Zr abundances than the adopted composition should be more appropriate.

By this evolutionary model, major-element mass balance calculations performed starting from the calc-alkaline basalts (e.g. SAR41) to several basaltic andesites and andesites (e.g. SAR119, SAR37, and SAR7) have provided satisfactory results (low ΣR^2 values). However, trace-element quantitative calculations show considerable differences between the modelled values and the observed ones for some incompatible elements (i.e. Rb, La, Ce, Zr,) (see the transition calc-alkaline basalt SAR41-basaltic andesite SAR119 in Table 4) that cannot be explained by crustal contamination. On the other hand, although the fractionation of accessory mineral phases such as zircon could account for most of the observed chemical variations, zircon crystallization appears unrealistic in similar basic magmas. Accordingly, the evolved types of the calc-alkaline suite (basaltic andesites, andesites, dacites) entail the occurrence of primary basic magmas, different from those that formed the sampled calc-alkaline basalts.

The high incompatible element (Rb, Zr, LREE) contents of the calc-alkaline basalt SAR41 cannot be produced by significant crustal contamination since SAR41 shows one among the lowest Sr isotopic composition values found in the calc-alkaline rocks. On the other hand, they could be better ascribed either to the mantle source and/or variable degrees of partial melting.

Sr and Nd isotopic data for the basic and intermediate dyke rocks are inconsistent with a depleted mantle source (Table 3, fig. 8) and suggest the addition of a crustal-type component. Quantitative modelling suggests that a process of combined assimilation and fractional crystallisation (AFC) could account for the Sr isotopic variations observed within the calc-alkaline dykes. Accordingly, the possibility that crustal contamination during the ascent of magmas to the surface could have significantly affected also the less evolved calc-alkaline rocks, modifying their original isotopic signatures, cannot be wholly ruled out since these rocks are not unfractionated mantle melts. Tholeiitic basalts are different from

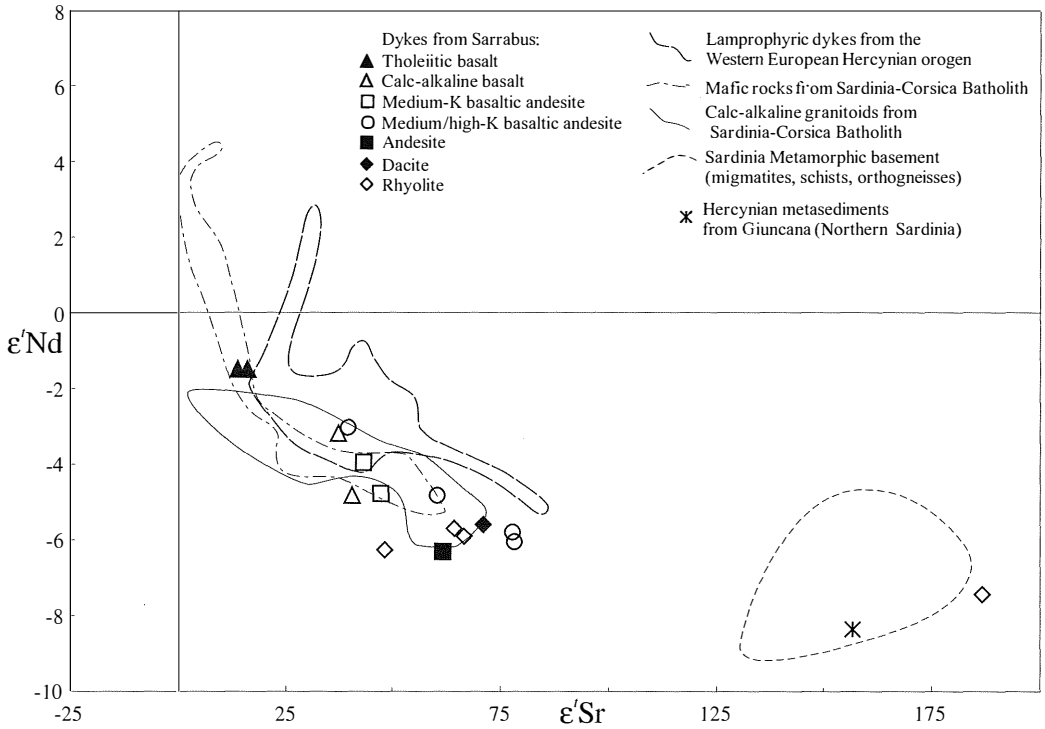

Fig. 8 – Nd and Sr epsilon values, corrected for decay, for selected dyke rocks from Sarrabus. Also shown are the isotopic data for the calc-alkaline products (mafic rocks and granitoids) of the Sardinia Corsica Batholith (data from Cocherie *et al.*, 1994 and Tommasini *et al.*, 1995); the late Carboniferous-lower Permian lamprophyres from the western European Hercynian Belt (data from Turpin *et al.*, 1988); the Hercynian metamorphic basement of Sardinia (data from Di Vincenzo *et al.*, 1996), the metasediments from Hercynian metamorphic basement from northern Sardinia (data from Del Moro, unpublished) used as contaminant in the AFC models. Symbols as in fig. 2.

other basic dyke rocks in having initial Sr and Nd isotopic ratios far less (0.70515 ÷ 0.70532) and greater (0.512215), respectively. Nevertheless, tholeiitic basalts might also have suffered a slight crustal contamination since none of them can be considered a primary mantle melt. However, as we already pointed out, systematic correlations between fractionation and Sr and Nd isotopic ratios seem to be lacking within ThB, in agreement with what was highlighted for the tholeiitic dykes from central and southern Sardinia (Traversa and Vaccaro, 1992). Thus, the negative ε^tNd and positive ε^tSr values of tholeiitic basalts could reflect the enriched character of the mantle source. Recycling of crustal materials through subduction process might cause the enrichment process. In fact, in comparison with a primordial mantle composition, the basic dyke rocks of Sarrabus show enrichements in LILE (Ba, Rb, Th, K, Pb) and LREE and marked Ti, Nb, P depletions, typical features of arc magmatism (Bailey, 1981; Pearce, 1982, 1983; Briqueu *et al.*, 1984) (fig. 9). An origin from a mantle source previously modified by recycling of crustal materials was also proposed for the transitional basaltic late-Hercynian dykes from central and northern Sardinia (Traversa and Vaccaro, 1992). Moreover, the existence of an Hercynian mantle enriched by subduction process was claimed for explaining the geochemical and isotopic features of other Carboniferous-Permian magmatic products: i.e.

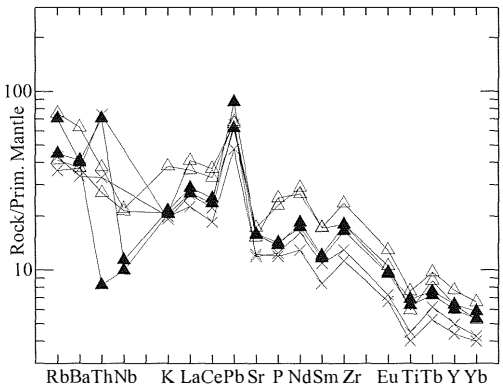

Fig. 9 – Primitive mantle-normalized trace element patterns for selected basic dyke rocks from Sarrabus. Normalizing values from Sun and Mc Donough (1989). Symbols: ▲ Tholeiitic dykes (ThB); △ calc-alkaline basaltic dykes (CaB); × high-Mg medium-K basaltic andesitic dykes.

the late-Carboniferous early Permian minette and kersantite dykes from the western European Hercynian belt (Turpin *et al.*, 1988); the quartz-diorites of Limousin (French Massif Central; Shaw *et al.*, 1993); the gabbros of Sardinia-Corsica Batholith (Tommasini *et al.*, 1995), the Permian magmatic products from the Alps area (Rottura *et al.*, 1997; 1998). Nevertheless, Cocherie *et al.* (1994), basing on the low $^{87}Sr/^{86}Sr_i$ (~ 0.704) and positive $\varepsilon'Nd$ (+0.2 ÷ +4.6) values and the trace element distribution shown by the most primitive tholeiitic and calc-alkaline mafic rocks from Corsica Hercynian Batholith, ruled out an enrichment of the mantle source related to subduction processes, and they ascribed the heterogeneous Sr and Nd isotopic signatures of the mafic suite to interaction with crustal fluids during fractional crystallization of mafic magma.

The two rock groups of felsic dykes (PR and MmPR) differ distinctly owing to their mineralogical and petrochemical features and Sr - Nd isotopic signatures.

PR dykes displays characters similar to those of S-type granites (Chappel and White, 1974), namely: presence of Al-silicates (Al-biotite, muscovite, garnet), ASI values always higher than 1.0 and frequently higher than 1.1; high K/Na, Rb/Sr and Rb/Ba ratios, Rb/Zr ratios greater than 3 like those of syn-orogenic granites (Harris *et al.*, 1986). For most PR samples, Zr, Th and REE contents are low, with very low LREE/HREE ratios. Their chemical composition and high Sr isotopic ratios (0.71548 ÷ 0.71731) are similar to those of other late-Hercynian peraluminous dykes from Sardinia (Vaccaro *et al.*, 1991; Traversa and Vaccaro, 1992) as well as those of syn-tectonic peraluminous monzogranites (A and D groups) cropping out in the migmatitic complex of the Tarra Padedda area (northern Sardinia) (Macera *et al.*, 1989), which are both believed to derive by partial melting from a metasedimentary crustal source (Macera *et al.*, 1989; Traversa and Vaccaro, 1992).

The other group of rhyolites (MmPR) is represented by metaluminous up to mildly peraluminous types that usually lack primary peraluminous silicates, apart from biotite. Generally, they are more enriched in Zr and LREE (La = 117 ÷ 225 × chondrite) than the PR dykes and they show fractionated REE patterns (La_n/Yb_n = 9 ÷ 14.4). Their Rb/Sr, Rb/Ba and Rb/Zr ratios display large variations (0.45 ÷ 8.5, 0.22 ÷ 1.2, 0.5 ÷ 1.8, respectively). The lowest values are clearly out of the typical range of magmas deriving from a metapelitic source (Miller, 1985; Harris *et al.*, 1986). This group of rhyolites shows initial $^{87}Sr/^{86}Sr$ ratios (0.70757 ÷ 0.70886) and $\varepsilon'Nd$ (-6.3 ÷ -5.7) values that partially overlap those of the calc-alkaline basic-intermediate dykes.

Some of the major and trace element variations observed within each rhyolite group could be ascribed to fractionation of plagioclase, biotite and some accessories such as apatite, monazite, allanite and zircon.

In order to evaluate the possibility of a genetic link between mafic and felsic dyke rocks by fractional crystallization processes, quantitative modelling was performed between the most evolved samples of the mafic suite (e.g. SAR7) and the rhyolite rocks. On the basis of major-element mass balance calculations, an origin by fractionation of amphibole+plagioclase+olivine+ilmenite+apatite

from the andesitic magmas seems to be numerically feasible only for some MmPR rocks (e.g. SAR131, SAR87; Table 4). Trace element modelling agrees with the results of the major-element calculations. Some differences between the calculated and observed values of Zr, La and Ce could be explained by the removal of accessory phases such zircon and allanite not included in the inferred fractionating assemblage. The slight Sr isotopic variation between the andesite sample SAR7 and the metaluminous rhyolite ones suggests no or only limited crustal contamination processes during the evolution of rhyolites. The different extent of crustal contamination, greater during the evolution from basaltic andesites to andesites and remarkably low in the transition from andesitic to rhyolitic melts, could be related to the decreasing heat budget of the system. Thus, it seems plausible that some rhyolites could derive through crystal fractionation from less evolved calc-alkaline types. However, the fractional crystallization model fails to replicate the high alkali contents (especially K_2O content) of the most silicic MmPR samples (e.g. SAR139; Table 4). Furthermore, suppose the rhyolites derived by crystal fractionation from mafic rocks, it is quite unusual that a mineral phase such as calcic amphibole, so abundant in the mafic dykes and that should be one of the main phases forming the fractionating assemblage, is wholly lacking in the rhyolites. Therefore, partial melting of the crust seems a likely origin not only for the peraluminous rhyolites but also for most metaluminous rhyolites. This hypothesis is also supported by the normative composition – close to that of minimum melt of the haplogranitic system – of the rhyolitic dyke rocks and by their incompatible element distribution typical of post-collision granites (fig. 10). It is worth noting that the group of MmPR dykes displays remarkable analogies, in term of major and trace element composition and Sr and Nd isotopic features, with the calc-alkaline granitoids from the Sardinia-Corsica Batholith (cp. Tommasini *et al.*, 1995) which are believed to be produced by crustal anatexis (Poli *et al.*, 1989). In particular, the MmPR types with the lowest SiO_2 and highest CaO contents (e. g. SAR131, SAR87), are similar to the late-tectonic monzogranites from the Sardinia-Corsica Batholith, whereas the more silicic MmPR rocks look like the post-tectonic leucogranites.

Thus, the differences in mineralogical, chemical and Sr-Nd isotopic features among the two groups of rhyolitic rocks could mainly reflect different crustal sources, as also proposed by Traversa and Vaccaro (1992) for the rhyolite dykes from central and northern Sardinia. The occurrence throughout Sardinia of rhyolite dykes with geochemical and Sr isotopic characteristics (Traversa and Vaccaro, 1992) similar to both the Sarrabus rhyolitic groups suggests a broad uniformity on a large scale of the crustal sources from which rhyolite dykes originated.

Sr and Nd isotopic data contribute to establishing the nature of potential crustal sources involved in the formation of felsic dyke rocks. In fig. 11, the initial Sr and Nd isotopic ratios of rhyolitic dykes are compared with the Sr-Nd isotopic evolution of various crustal materials. For the Sardinia-Corsica sector, only isotopic data of micaschistes, migmatites,

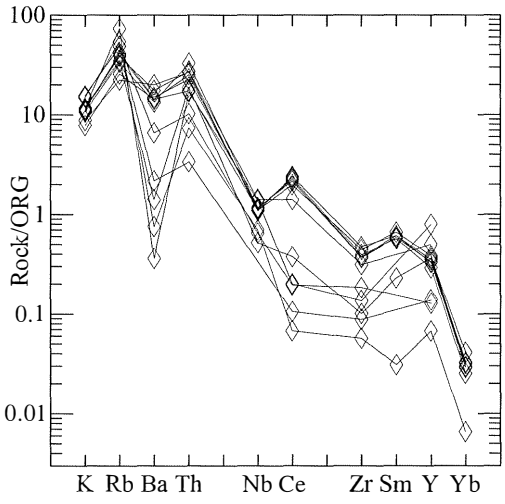

Fig. 10 – ORG-normalized trace element patterns for selected rhyolitic dyke rocks from Sarrabus. Normalizing values from Pearce *et al.*, (1984).

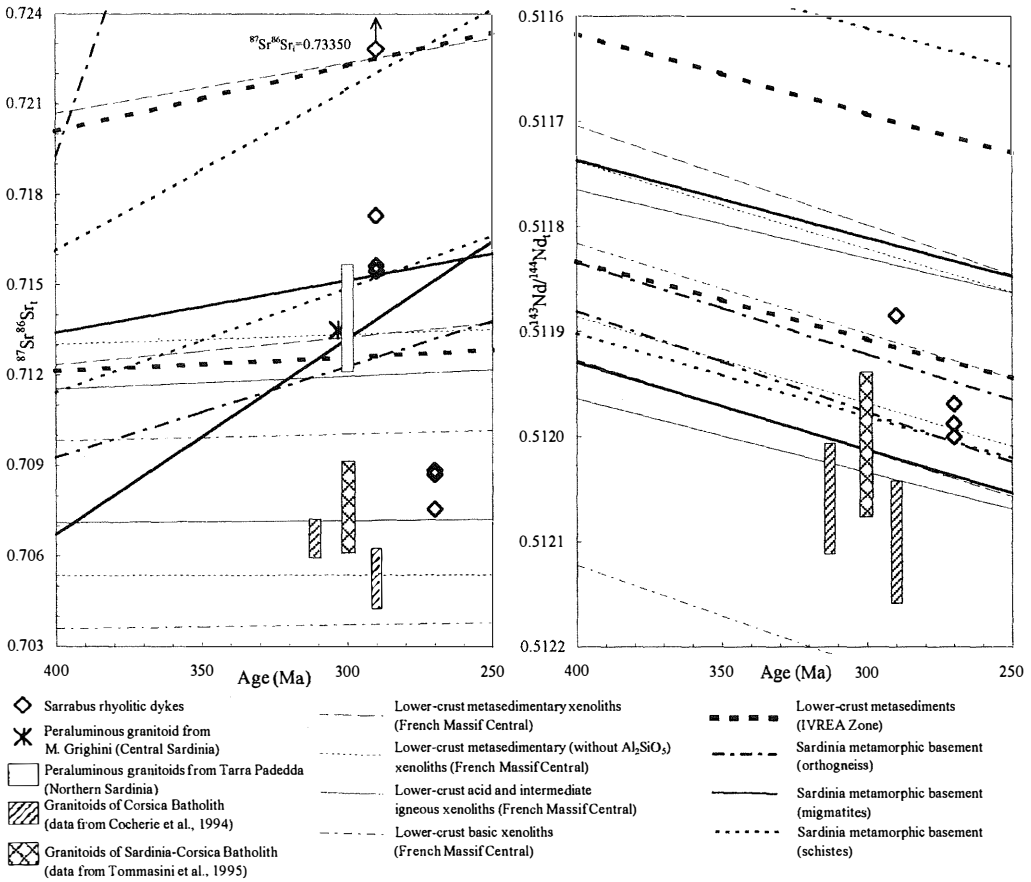

Fig. 11 – Initial Sr and Nd isotopic ratios for selected rhyolitic dykes from Sarrabus compared with the isotopic evolution of potential crustal sources. Line pairs represent upper and lower limits of the isotopic range of various crustal materials. Data are from lower crustal xenoliths of the French Massif Central (Downes *et al.*, 1990), metasediments of the Ivrea Zone (Voshage *et al.*, 1990) and Hercynian metamorphic basement of Sardinia (Di Simplicio *et al.*, 1974; Ferrara *et al.*, 1978; Di Vincenzo *et al.*, 1996). The isotopic compositions of granitoids from the Sardinia Corsica Batholith (data from Carmignani *et al.*, 1985; Macera *et al.*, 1989; Cocherie *et al.*, 1994; Tommasini *et al.*, 1995) are also shown for comparison.

augengneisses and orthogneisses from the metamorphic basement are available (Di Simplicio *et al.*, 1974; Ferrara *et al.*, 1978; Di Vincenzo *et al.*, 1996) whereas information on the lower-crust components is lacking. Thus, Sr and Nd isotopic ratios of lower-crust lithologies from the French Massif Central (Downes *et al.*, 1990) and from the Ivrea Zone (Voshage *et al.*, 1990) are reported, also considering that, according to paleogeographic reconstructions (Westphal *et al.*, 1976; Arthaud and Matte, 1977a; Edel *et al.*, 1981), during the late Paleozoic, the Sardinia-Corsica microplate was close to the southern France.

PR dykes show $(^{87}Sr/^{86}Sr)_t$ values comparable or slightly higher than those of the peraluminous granitoids from Tarra Padedda (Macera *et al.*, 1989) and from Mt. Grighini – Central Sardinia (Carmignani *et al.*, 1985). Moreover, Sr and Nd isotopic data of the PR dykes well match those of the micaschists from the Sardinia metamorphic basement (Di Vincenzo *et al.*, 1996) as well as those of granulite- and amphibolite-facies metapelites

from the lower crust of the Ivrea zone (Voshage *et al*., 1990) and those of lower crust granulitic metasedimentary xenoliths from the French Massif Central (Downes *et al*., 1990) (fig. 11). Pelitic metasedimentary crustal levels seem to therefore be the most suitable protolith of PR dykes.

The MmPR dykes have a Sr and Nd isotopic composition similar to that of the calc-alkaline granitoids from the Sardinia-Corsica Batholith (Cocherie *et al*., 1994; Tommasini *et al*., 1995). Sr isotopic ratios are lower than those of metasedimentary crustal rocks and overlap those of acid/intermediate igneous and basic/ultramafic xenoliths. On the other hand, Nd isotope composition is compatible with different protoliths, metasedimentary as well metaigneous. These isotopic data lead us to rule out an origin from a pure pelitic sedimentary protolith and suggest the additional involvement of a juvenile mantle component. Processes of mixing, hybridization and assimilation between mantle-derived magmas and crustal melts/rocks can be considered to explain the hybrid Sr and Nd isotopic composition of rhyolitic magmas. Since rhyolitic dyke rocks show no field and petrographic evidence of interaction between mafic and felsic magmas, the eventual mixing and/or assimilation processes might take place only in the lower crust, when magma was forming. Studies on granulitic xenoliths from the French Massif Central (Downes *et al*., 1990) and on outcrops of the Hercynian basement in the Ivrea Zone (Voshage *et al*., 1990) provide indications for a deep interaction between mantle and crustal components in the lower crust of the Hercynian belt as a result of underplating and intraplating of mantle-derived basic magma during the Hercynian time. Melting of hybrid metaigneous crustal material may also produce acid melts with barely evolved Sr and Nd isotopic compositions. Partial melting of basic-intermediate metaigneous sources was proposed by Tommasini *et al*. (1995) for the genesis of I-type granitoids from the Sardinia-Corsica Batholith. These crustal sources might have formed by underplating of mantle-derived magmas, during the Ordovician calc-alkaline igneous activity. In effect, the close resemblance in terms of geochemical and isotopic features between MmPR dykes and the granitoids from the Sardinia-Corsica Batholith suggests that the two types of rocks could be derived from the same crustal sources.

Concluding remarks

The late-Hercynian dyke magmatism of Sarrabus occurred after the emplacement of the SE Sardinia Hercynian granitoids (311-295 Ma), during a post-collisional phase, rapidly evolving from orogenic to anorogenic settings. Dyke swarms were intruded in a time span between about 290 and 260 Ma, as suggested by Rb-Sr mica ages obtained on Sarrabus dyke rocks. The Rb-Sr mica ages and the sequence of felsic and mafic products are similar to those previously recognized in other areas of Sardinia and southern Corsica. The early intrusions are dated around 290 Ma and are represented by few small peraluminous muscovite-bearing rhyolitic dykes. Swarms of thick rhyolitic dykes (granite porphyries, microgranites and aplites) emplaced later (~270 Ma). According to field and geocronological data (259 Ma), the emplacement of the basic and intermediate dykes, mainly consisting of basaltic andesites and andesites, was generally subsequent to that of the felsic dykes. Minor basaltic dykes of tholeiitic affinity could represent the final events possibly related to the late-Permian basaltic dyke activity.

Petrography, mineral and whole-rock chemistry, Sr and Nd isotopic data indicate that mafic dykes were mantle-derived, although the least evolved basic rocks also suffered minor crystal fractionation.

Major and trace element modelling demonstrates that fractional crystallization and simultaneous assimilation of metasedimentary material (AFC process) controlled the evolution from the least evolved to the most evolved rocks of the calc-alkaline suite. As

inferred from AFC modelling, the assimilation of ~ 12-13 wt% crustal materials can account for the increasing $^{87}Sr/^{86}Sr_t$ and decreasing $\varepsilon'Nd$ values in the evolution from basic to intermediate types.

The calc-alkaline basaltic dykes are enriched in some incompatible elements (i.e. Rb, La, Ce, and Zr) compared with the high-Mg basaltic andesites. Taking into account the relatively low initial $^{87}Sr/^{86}Sr$ ratios of the calc-alkaiine basalts, these enrichments, cannot be explained by crustal contamination process but suggest the occurrence of different calc-alkaline primary magmas related to different mantle sources and/or different melting conditions.

The parent magmas of the least evolved Sarrabus basic dyke rocks, as well as those of the late-Hercynian calc-alkaline and tholeiitic dykes from other sectors of Sardinia, are suggested to have derived from a mantle source enriched in LILE and LREE. These characters could be possibly attributed to metasomatic processes of the lithospheric mantle during previous subduction events.

Among the felsic dykes, a group of muscovite bearing rhyolites (PR group), besides the peraluminous character, shows high K/Na, Rb/Sr and Rb/Ba ratios, high $(^{87}Sr^{86}Sr)_t$ and low $\varepsilon'Nd$ values [$(^{87}Sr/^{86}Sr)_t = 0.71548 \div 0.73350$, $\varepsilon'Nd = -7.45$] strongly suggesting for these rhyolitic rocks an origin by partial melting of metasedimentary pelitic sources. The remaining rhyolites (MmPR group) are metaluminous to mildly peraluminous and display an Sr and Nd isotopic composition close to that of the most evolved calc-alkaline dyke rocks. This fact could suggest a genetic link between rhyolites and calc-alkaline basic-intermediate rocks. However, major and trace element mass balance calculations support an origin by a crystal fractionation process only for the least silicic MmPR rocks. Therefore, partial melting of crustal sources appears to be a more plausible origin for most of the MmPR rhyolites. The relatively low $(^{87}Sr/^{86}Sr)_t$ ($0.70757 \div 0.70886$) and high $\varepsilon'Nd$ ($-5.7 \div -6.3$) values entail the participation of a mantle component and could suggest metaigneous basic-intermediate sources for the genesis of this group of rhyolites.

APPENDIX

Analytical procedures

Major and trace element compositions of whole-rocks were determined by XRF, except for MgO and Na_2O (AAS determination), FeO (wet chemical titration) and L.O.I. (loss on ignition by standard gravimetric techniques). The XRF analyses were carried out at the Dipartimento di Scienze della Terra - Università di Perugia, on a Phillips PW1400 automatic spectrometer following the method of Franzini and Leoni (1972) and that of Kaye (1965) for major and trace elements, respectively.

Sm and Nd concentrations, as REEs, were detected by the ICP-MS method at the CRPG laboratory of Nancy (France). Sr and Nd isotope analyses were performed at the Istituto di Geocronologia e Geochimica Isotopica - CNR of Pisa (Italy). Rb, Sr and REE were purified using standard cation exchange procedures. Nd was separated from other REEs using an 8×0.3 cm column filled with Teflon powder coated with di-2-ethil-hexil hydrogen phosphate. Rb and Sr contents were measured by the isotopic dilution method. Rb determination was carried out on a single collector Finnigan MAT TH5 mass spectrometer. For mineral concentrates, Sr concentration and isotopic composition analyses were performed on a VG-54E Isomass single collector mass spectrometer. Sr and Nd isotopic ratios of whole-rock samples were measured on a Finnigan MAT-262 multicollector mass spectrometer. Measured total blanks were <2ng for Sr and <0.1 ng for Nd. Sr and Nd isotopic ratios were adjusted to a value of $^{87}Sr/^{86}Sr = 0.71025$ for NBS987 and of $^{143}Nd/^{144}Nd = 0.51185$ for La Jolla standards, respectively. During the period of isotopic analyses, replicate measurements of the NBS987 standard gave the average values of $^{87}Sr/^{86}Sr = 0.710275 \pm 6$ ($\pm 2\sigma$, $n = 41$) on VG-54E mass spectrometer and $^{87}Sr/^{86}Sr = 0.710246 \pm 3$ ($\pm 2\sigma$, $n = 33$) on Finnigan MAT-262 mass spectrometer. Replicate measurements of the La Jolla standard gave average value of $^{143}Nd/^{144}Nd = 0.511849 \pm 1$ ($\pm 2\sigma$, $n = 37$) on Finnigan MAT-262 mass spectrometer. The estimated errors for $^{87}Rb/^{86}Sr$ and $^{147}Sm/^{144}Nd$ ratios are 1% and 7%, respectively. Isochrons were calculated by Isoplot software (Ludwig, 1990).

ACKNOWLEDGMENTS

This work is part of a research program supported by the Italian MURST 40% and CNR grants (to G. Traversa). We thank G. De Grandis and C. Quercioli for their assistance during mineral separation procedures, U. Giannotti and G. Pardini for help during the instrumental work. Helpful comments by R. Petrini and an anonimous reviewer are gratefully acknowledged.

REFERENCES

ARTHAUD F. and MATTE PH. (1975) — *Les décrochments tardihercyniens du sud-ouest de l'Europe. Géométrie et essai de reconstruction des conditions de déformation.* Tectonophysics, **25**, 131-171.

ARTHAUD F. and MATTE PH. (1977a) – *Synthèse provisoire sur l'evolution tectonique et les raccords entre les segments hercyniens situés autour du bassin nord-Baléare (Sud de la France, Espagne, bloc corso-sarde).* Coll. Int. CNRS (Rennes), **243**, 497-513.

ARTHAUD F. and MATTE PH. (1977b) — *Late Paleozoic strike slip faulting in southern Europe and northern Africa: Results of a lateral shear-zone between the Appalachians and the Urals.* Geol. Soc. Am. Bull., **88**, 1305-1320.

ATZORI P. and TRAVERSA G. (1986) — *Post-granitic permotriassic dyke magmatism in eastern Sardinia (Sarrabus p.p., Barbagia, Mandrolisai, Goceano, Baronie and Gallura).* Per. Mineral., **55**, 203-231.

BAILEY J.C. (1981) — *Geochemical criteria for a refined tectonic discrimination of orogenic andesites.* Chem. Geol., **32**, 139-154.

BALDELLI C., BIGAZZI G., ELTER F.M. and MACERA P. (1986) - *Description of a permo-trias alkaline lamprophyre embedded into the micaschists of garnet-staurolite-kyanite grade north-eastern Sardinia island.* Meeting Paleozoic, stratigraphy, tectonics, metamorphism and magmatism in Italy, (Siena, december 13-14, 1986).

BOYNTON W.V. (1984) – *Cosmochemistry of the Rare earth Elements: meteorite studies.* In: HENDERSON P. (Ed.), «Rare Earth Element Geochemistry», Elsevier, 63-107.

BRIQUEU L., BOUGAULT H. and JORON J.L. (1984) — *Quantification of Nb, Ti and V anomalies in magmas associated with subduction zones: petrogenetic implications.* Earth Planet. Sci. Lett., **68**, 297.

BROTZU P., CALLEGARI E. and SECCHI A. (1993) — *The search for the parental magma of the high-K calc-alkaline igneous rock series in the southernmost Sardinia Batholith.* Per. Mineral., **63**, 253-280.

BROTZU P., FERRINI V. and MASI U. (1983) — *Stable-isotope geochemistry of Hercynian granitoid rocks from the Sarrabus massif (Southeastern Sardinia, Italy).* Isotope Geoscience, **1**, 77-90.

BROTZU P. and MORBIDELLI L. (1974) – *Lineamenti petrografici e geostrutturali di un settore del Sarrabus meridionale (Sardegna sud-orientale).* Atti Acc. Naz. Lincei Serie VIII, **XII**(1).

BROTZU P., MORBIDELLI L. and TRAVERSA G. (1978) – *Caratteri petrografici e chimici delle sieniti del Sarrabus meridionale (Sardegna sud-orientale).* Per. Mineral., **47**, 83-98.

CARMIGNANI L., DEL MORO A., FRANCESCHELLI M., GHEZZO C. and PERTUSATI P.C. (1985) — *Sistematica Rb-Sr dei graniti sincinematici del M.te Grighini, Sardegna Centrale. In: Evoluzione stratigrafica, tettonica, metamorfica e magmatica del Paleozoico italiano.* Siena, Riunione Scientifica, December 13-14, 61-63.

CARMIGNANI L., COCOZZA T., GHEZZO C., PERTUSATI P.C. and RICCI C.A. (1987) — *Structural model of the Hercynian basement of Sardinia.* CNR Progetto finalizzato geodinamica, sottoprogetto 5.

CAROSI R., GATTIGLIO M., MUSUMECI G. and OGGIANO G. (1992) —*Geologia della catena ercinica in Sardegna – Zona a falde.* In: CARMIGNANI L., PERTUSATI P.C., BARCA S., CAROSI R., DI PISA A., GATTIGLIO M., MUSUMECI G. and OGGIANO G. (Eds.), «Struttura della Catena Ercinica in Sardegna», 77-145.

CHAPPELL B.W. and WHITE A. J.R. (1974) — *Two contrasting granite types.* Pac. Geol., **8**, 173-174.

COCHERIE A., ROSSI PH., FOUILLAC A.M. and VIDAL PH. (1994) — *Crust and mantle contributions to granite genesis - An example from the Variscan batholith of Corsica, France, studied by trace element and Nd-Sr-O-isotope systematics.* Chem. Geol., **115**, 173-211.

DE LA ROCHE H., LETERRIER J., GRANDCLAUDE P., MARCHAL M. (1980) — *A classification of volcanic and plutonic rocks using R1-R2 diagram and major element analysis. Its relationships with current nomenclature.* Chem. Geol., **29**, 183-200.

DEL MORO A., DI PISA A. and OGGIANO G. (1996) — *Relationship between an autunian volcano-sedimentary succession and the Tempio Massif granites (northern Sardinia). Geochronology and field constraints.* Plinius, **16**, 94-95.

DE PAOLO D.J. (1981) – *Trace element and isotopic effects of combined wallrock assimilation and fractional crystallisation.* Earth Planet. Sci. Lett., **53**, 189-202.

DI SIMPLICIO P., FERRARA G., GHEZZO C., GUASPARRI G., PELLIZZER R., RICCI C.A., RITA F. and SABATINI G. (1974) — *Il metamorfismo e il magmatismo paleozoico della Sardegna.* Rend. S.I.M.P., **30**, 979-1068.

DI VINCENZO G., GHEZZO C. and TONARINI S. (1994) — *Geochemistry and Rb-Sr geochronology of the Hercynian peraluminous Sos Canales pluton (central Sardinia, Italy).* C.R. Acad. Sci. Paris 319, **II**, 783-790.

DI VINCENZO G., ANDRIESSEN P.A. and GHEZZO C. (1996) — *Evidence of two different components in a Hercynian peraluminous cordierite-bearing granite: the San Basilio intrusion (Central Sardinia, Italy).* J. Petrol., **37**, (5), 1175-1206.

DOWNES H., DUPUY C. and LEYRELOUP A.F. (1990) — *Crustal evolution of the Hercynian belt of Western Europe: evidence from lower-crustal granulitic xenoliths (French, Massif Central).* Chem. Geol., **83**, 209-231.

EDEL J.B., MONTIGNY R. and THUIZAT R. (1981) — *Late Paleozoic rotations of Corsica and Sardinia: New evidence from paleomagnetic and K-Ar studies.* Tectonophysics, **79**, 201-223.

FAURE G. (1986) — *Principles of isotope geology.* John Wiley and Sons, New York, pp. 589.

FERRARA G., RICCI C.A and RITA F. (1978) — *Isotopic ages and tectonometamorphic history of the metamorphic basement of north-eastern Sardinia.* Contrib. Mineral. Petrol., **68**, 99-106.

FRANZINI M. and LEONI L. (1972) — *A full matrix correction in X-ray fluorescence analysis of rock samples.* Atti Soc. Tosc. Sc. Nat., Pisa, Mem., **79** (Serie A), 7-22.

HÄNNY R., GRAUERT B. and SOPTRAJANOVA G. (1975) — *Paleozoic migmatites affected by high-grade Tertiary metamorphism in the Central Alps (Valle Bodengo, Italy).* Contrib. Mineral. Petrol., **51**, 173-196.

HARRIS N.B.W., PEARCE J.A. and TINDLE A.G. (1986) — *Geochemical characteristic of collision-zone magmatism.* In: COWARD M.P. and RIES A.C. (Eds.)., *Collision tectonics.* Geol. Soc. Spec. Pub., **19**, 67-81.

HENDERSON P. (1986) — *Inorganic geochemistry.* Pergamon Press, Oxford, pp. 353.

JACOBSEN S.B. and WASSERBURG G.J. (1984) — *Sm-Nd isotopic evolution of chondrites and achondrites, II.* Earth Planet. Sci. Lett., **67**,137-150.

KAYE M.J. (1965) — *X-ray fluorescence determination of several trace elements in some standard geochemical samples.* Geochim. Cosmochim. Acta, **29**, 139-142.

LUDWIG K.R. (1990) - *ISOPLOT: a plotting and regression program for radiogenic isotope data, IBM-PC compatible computers, Version 2.02.* US Geological Survey, Open-File Report, 88-557.

MACERA P., CONTICELLI S., DEL MORO A., DI PISA A., OGGIANO G. and SQUADRONE A. (1989) — *Geochemistry and Rb/Sr age of syn-tectonic peraluminous granites of Western Gallura, Northern Sardinia: constraints on their genesis.* Per. Mineral., **58**, 25-43.

MILLER C.F. (1985) – *Are strongly peraluminous magmas derived from pelitic sedimentary sources?* J. Geology., **93**, 673-689.

MITTLEFEHLD D.W. and MILLER C.F. (1983) — *Geochemistry of the Sweetwater W-ash pluton, California: implication for «anomalous» trace element behaviour during differentiation of felsic magmas.* Geochim. Cosmochim. Acta, **47**, 109-124.

MIYASHIRO A. (1974) — *Volcanic rock series in island arcs and active continental margins.* Am. J. Sci., **274**, 321-355.

NIELSEN R. (1998) — *References and values for mineral-melt and mineral –fluid partition coefficients.* Web page and FTP access to the site: www.ep.llnl.gov/germ/partitioning.html.

NICOLETTI M., ARDANESE L.R. and COLASANTE S. (1982) — *La granodiorite di Capo Carbonara (Sardegna, Italia). Età Kr-Ar di fasi minerali in paragenesi.* Rend. S.I.M.P., **38**, 765-769.

NOVI A. (1995) - Studio geocronologico delle vulcaniti tardo-palozoiche sarde dei settori settentrionale (Gallura) e centro-orientale (Area di Galtellì). Tesi di laurea, Università di Pisa, 218 pp.

PASQUALI C. and TRAVERSA G. (1996) – *Petrography and mineral chemistry of late-Hercynian dykes from southern Corsica.* Per. Mineral., **65**, 213-256.

PASQUALI C. (1998) – *Petrologia del magmatismo filoniano tardo-ercinico della Corsica meridionale.* Tesi di Dottorato, Università degli Studi di Perugia.

PEARCE J.A. (1982) - *Trace elements characteristics of lavas from destructive plate boundaries.* In: THORPE R.S. (Ed.), Andesites, John Wiley and sons, New York, 525-548.

PEARCE J.A. (1983) — *The role of sub-continental litosphere in magmas genesis at destructive plate margins.* In: HAWKESWORTH C.J. and NORRY M.J. (eds.), «Continental Basalts and Mantle Xenoliths», Nantwich: Shiva Publications, 230-249.

PEARCE J.A., HARRIS N.B.W. and TINDLE A.G. (1984) — *Trace element discrimination diagrams for the tectonic interpretation of granitic rocks.* J. Petrol., **25**, 956-983.

PECCERILLO A. and TAYLOR S.R. (1976) — *Geochemistry of eocene calc-alkaline volcanic from the Kastamonu area, northern Turkey.* Contrib. Mineral. Petrol., **58**, 63-81.

PERFIT M.R., GUST D.A., BENCE A.E., ARCULUS R.J. and TAYLOR S.R. (1980) — *Chemical characteristics of island arc basalts: implications for mantle sources.* Chem. Geol., **30**, 227-256.

PIRINU M.N. (1991) – *Le sieniti del Sarrabus meridionale.* Tesi di dottorato, Università di Napoli.

PIRINU M.N., BROTZU P., CALLEGARI E. and SECCHI F. (1996) – *Age and field relationships of albite-rich monzosyenite intruded into the Sarrabus granitoids (SE Sardinia, Italy).* Per. Mineral., **65**, 289-304.

POLI G.P., GHEZZO C. and CONTICELLI S. (1989) — *Geochemistry of the granitic rocks from the Hercynian Sardinia-Corsica batholith: implication for magma genesis.* Lithos, **23**, 247-266.

RONCA S. (1996) – *Petrologia del magmatismo filoniano tardo-ercinico del Sarrabus (Sardegna sud-orientale).* Tesi di Dottorato, Università degli Studi di Perugia.

RONCA S. and TRAVERSA G. (1996) — *Late-Hercynian dyke magmatism of Sarrabus (SE Sardinia).* Per. Mineral., **65**, 35-70.

ROTTURA A., DEL MORO A., CAGGIANELLI A., BARGOSSI G.M. and GASPAROTTO G. (1997) — *Petrogenesis of the Monte Croce granitoid in the context of the Permian magmatism of southern Alps, Italy.* Eur. J. Mineral., **9**, 1293-1310.

ROTTURA A., BARGOSSI G.M., CAGGIANELLI A., DEL MORO A., VISONÀ D. and TRANNE C.A. (1998) — *Origin and significance of the Permian high-K magmatism in the central-eastern southern Alps, Italy.* Lithos, **45**, 329-348.

SALLEBY J. and SHARP W. (1978) — *Preliminary report on the behaviour of U-Pb zircon and K-Ar systems in polymetamorphosed ophiolitic rocks ang batholithic rocks, Southwestern Sierra Nevada foothills, California.* In: ZARTMAN R.E. (ed.), «Short papers of the Fourth International Conference on geochronology, cosmochronology , isotope geology», U.S. Geological Survey, 375-376.

SHAND S.J. (1949) – *Eruptive rocks.* Wiley, New York.

SHAW A., DOWNES H. and THIRLWALL M.F. (1993) — *The quartz-diorites of Limousin: elemental and isotopic evidence for Devono-Carboniferous subduction in the Hercynian belt of the French Massif Central.* Chem. Geol., **107**, 1-18.

STORMER JR. and NICHOLLS JC. (1978) – *XLFRAC a programme for interactive testing of magmatic differentiation model.* Comp. Geosci., **4**, 143-159.

SUN S.S. and MC DONOUGH W.F. (1989) – *Chemical and isotopic systematics of oceanic basalts: implications for mantle composition and processes. Magmatism in the Ocean Basins.* A.D. Saunders and M. J. Norry, (eds.), Geol. Soc. Lond. Spec. Publ., 331-345.

TOMMASINI S. (1993) - *Petrologia del magmatismo calcalcalino del batolite sardo-corso: processi genetici ed evolutivi dei magmi in aree di collisione continentale e implicazioni geodinamiche.* Tesi di Dottorato, Università di Perugia.

TOMMASINI S., POLI G. and HALLIDAY A.N. (1995) — *The role of sediment subduction and crustal growth in Hercynian plutonism: isotopic and trace element evidence from the Sardinia-Corsica batholith.* J. Petrol., **35** (5), 1305-1332.

TRAVERSA G. (1969) – *Sulla giacitura ed età di alcuni filoni basici nelle vulcaniti ignimbritiche permiane della Gallura (Sardegna settentrionale).* Rend. S.I.M.P., **25**, 149-155.

TRAVERSA G., VACCARO C., PASQUALI C., PENSI S. and RONCA S. (1991) — *Geological and structural features of late Hercynian dykes from Concas massif (NE Sardinia).* Congresso su Magmatismo basico e sorgenti di mantello: aspetti petrologici e geodinamici. S.I.M.P.-E.J.M., Plinius, **6**, 217.

TRAVERSA G. and VACCARO C. (1992) — *REE distribution in the late hercynian dykes from Sardinia.* IGCP n. 276, Newsletter, Vol. 5, Siena 1992, 215-226.

TRAVERSA G., RONCA S. and PASQUALI C. (1997) — *Post-Hercynian basic dyke magmatism of the Concas-Alà dei Sardi alignment (Northern Sardinia – Italy).* Per. Mineral., **66**, 233-262.

TURPIN L., VELDE D. and PINTE G. (1988) — *Geochemical comparison between minettes and kersantites from the Western European Hercynian orogen: trace element and Pb-Sr-Nd isotope constraints on their origin.* Earth Planet. Sci. Lett., **87**, 73-86.

VACCARO C. (1990) — *Magmatismo filoniano Carbonifero-Permiano della Sardegna: considerazioni geologiche, petrologiche e geocronologiche.* Tesi di Dottorato, Consorzio Università di Napoli-Catania.

VACCARO C., ATZORI P., DEL MORO A., ODDONE M., TRAVERSA G. and VILLA I. (1991) — *Geochronology and Sr Isotope geochemistry of late-hercynian dykes from Sardinia.* Schweitz. Mineral. Petrogr. Mitt., **71**, 221-230.

VOSHAGE H., HOFMANN A.W., MAZZICCHELLI M., RIVALENTI G., SINIGOI S., RACZEK I. and DEMARCHI G. (1990) — *Isotope evidence from the Ivrea Zone for a hybrid lower crust formed by magmatic underplating.* Nature, **347**, 731-736.

WESTPHAL M., ORSINI J. and VELLUTINI P. (1976) — *Le microcontinent corso-sarde, sa position initiale: données paléomagnétiques et raccords géologiques.* Tectonophysics, **30**, 141-157.

YURIMOTO H., DUKE E.F., PAPIKE J.J. and SHEARER CK. (1990) — *Are discontinuous chonrite-normalized REE patterns in pegmatitic granite system the results of monazite fractionation?*. Geochim. Cosmochim. Acta, **54**, 2141-2145.

ZEN E-A (1986) — *Aluminum enrichment in silicate melts by fractional crystallization: some mineralogic and petrographic constraints*. J. Petrol., **27**, 1095-1117.

ZHAO X.J. and COOPER J.A. (1993) — *Fractionation of monazite in the development of V-shaped REE patterns in leucogranite system: evidence from a muscovite leucogranite body in central Australia.* Lithos, **30**, 23-32.